WT-1330(EX)
EXTRACTED VERSION

OPERATION REDWING—PROJECT 5.4

In-Flight Participation of a B-57B

H. M. Wells, Jr.
D. M. Roha
D. V. Sallis
J. V. Ward
Wright Air Development Division
Wright-Patterson Air Force Base
Dayton, OH

The Martin Company
Baltimore, MD

28 July 1960

NOTICE:
This is an extract of WT-1330, Operation REDWING, Project 5.4.

Approved for public release;
distribution is unlimited.

Extracted version prepared for
Director
DEFENSE NUCLEAR AGENCY
Washington, DC 20305-1000

1 September 1985

Destroy this report when it is no longer needed. Do not return to sender.

PLEASE NOTIFY THE DEFENSE NUCLEAR AGENCY, ATTN: STTI, WASHINGTON, DC 20305-1000, IF YOUR ADDRESS IS INCORRECT, IF YOU WISH IT DELETED FROM THE DISTRIBUTION LIST, OR IF THE ADDRESSEE IS NO LONGER EMPLOYED BY YOUR ORGANIZATION.

UNCLASSIFIED

SECURITY CLASSIFICATION OF THIS PAGE

AD-A995446

REPORT DOCUMENTATION PAGE

1a. REPORT SECURITY CLASSIFICATION UNCLASSIFIED	1b. RESTRICTIVE MARKINGS
2a. SECURITY CLASSIFICATION AUTHORITY N/A since Unclassified	3. DISTRIBUTION/AVAILABILITY OF REPORT Approved for public release; distribution is unlimited.
2b. DECLASSIFICATION/DOWNGRADING SCHEDULE N/A since Unclassified	
4. PERFORMING ORGANIZATION REPORT NUMBER(S)	5. MONITORING ORGANIZATION REPORT NUMBER(S) WT-1330 (EX)
6a. NAME OF PERFORMING ORGANIZATION The Martin Company 6b. OFFICE SYMBOL (If applicable)	7a. NAME OF MONITORING ORGANIZATION Defense Atomic Support Agency
6c. ADDRESS (City, State, and ZIP Code) Baltimore, MD	7b. ADDRESS (City, State, and ZIP Code) Washington, DC
8a. NAME OF FUNDING/SPONSORING ORGANIZATION 8b. OFFICE SYMBOL (If applicable)	9. PROCUREMENT INSTRUMENT IDENTIFICATION NUMBER
8c. ADDRESS (City, State, and ZIP Code)	10. SOURCE OF FUNDING NUMBERS PROGRAM ELEMENT NO. / PROJECT NO. / TASK NO. / WORK UNIT ACCESSION NO.

11. TITLE (Include Security Classification)
OPERATION REDWING—PROJECT 5.4
In-Flight Participation of a B-57B, Extracted Version

12. PERSONAL AUTHOR(S)
Wells, H.M., Jr.; Roha, D.M.; Sallis, D.V.; and Ward, J.V.

13a. TYPE OF REPORT	13b. TIME COVERED FROM _____ TO _____	14. DATE OF REPORT (Year, Month, Day)	15. PAGE COUNT
		600728	62

16. SUPPLEMENTARY NOTATION This report has had sensitive military information removed in order to provide an unclassified version for unlimited distribution. The work was performed by the Defense Nuclear Agency in support of the DoD Nuclear Test Personnel Review Program.

17. COSATI CODES		
FIELD	GROUP	SUB-GROUP
18	3	
1	3	

18. SUBJECT TERMS (Continue on reverse if necessary and identify by block number)
Redwing, Project 5.4
B-57B Aircraft
Blast Effects (Aircraft)

19. ABSTRACT (Continue on reverse if necessary and identify by block number)

Project 5.4 was established to determine the response of the B-57 aircraft structure in-flight to thermal, gust, and overpressure effects of large-yield nuclear explosions primarily for the purpose of defining the delivery capabilities of the aircraft and secondarily to obtain basic information relative to the thermoelastic response of the aircraft structure.

The aircraft was instrumented to measure the overpressure, gust, and thermal inputs, and the response of various components of the structure to these inputs. The maximum skin temperature of 400F was the criterion for determination of the amount of thermal radiation which the B-57B could absorb without sustaining permanent buckling of the skin, and 600F was the criterion for the maximum safe limit. In thermally critical participations, the aircraft was normally positioned for the 400-degrees limit for the design yield and for less than 600 degrees for the positioning yield.

The data obtained during this project will provide (1) valuable design criteria data for

20. DISTRIBUTION/AVAILABILITY OF ABSTRACT	21. ABSTRACT SECURITY CLASSIFICATION
☒ UNCLASSIFIED/UNLIMITED ☐ SAME AS RPT ☐ DTIC USERS	UNCLASSIFIED
22a. NAME OF RESPONSIBLE INDIVIDUAL MARK D. FLOHR	22b. TELEPHONE (Include Area Code) 202-325-7559 / 22c. OFFICE SYMBOL DNA/ISCM

DD FORM 1473, 84 MAR 83 APR edition may be used until exhausted. All other editions are obsolete.

SECURITY CLASSIFICATION OF THIS PAGE

UNCLASSIFIED

19. ABSTRACT (Continued)

future aircraft, and (2) a basis for the verification and/or correction of present methods of predicting weapon effects in space and on aircraft structures.

FOREWORD

Classified material has been removed in order to make the information available on an unclassified, open publication basis, to any interested parties. The effort to declassify this report has been accomplished specifically to support the Department of Defense Nuclear Test Personnel Review (NTPR) Program. The objective is to facilitate studies of the low levels of radiation received by some individuals during the atmospheric nuclear test program by making as much information as possible available to all interested parties.

The material which has been deleted is either currently classified as Restricted Data or Formerly Restricted Data under the provisions of the Atomic Energy Act of 1954 (as amended), or is National Security Information, or has been determined to be critical military information which could reveal system or equipment vulnerabilities and is, therefore, not appropriate for open publication.

The Defense Nuclear Agency (DNA) believes that though all classified material has been deleted, the report accurately portrays the contents of the original. DNA also believes that the deleted material is of little or no significance to studies into the amounts, or types, of radiation received by any individuals during the atmospheric nuclear test program.

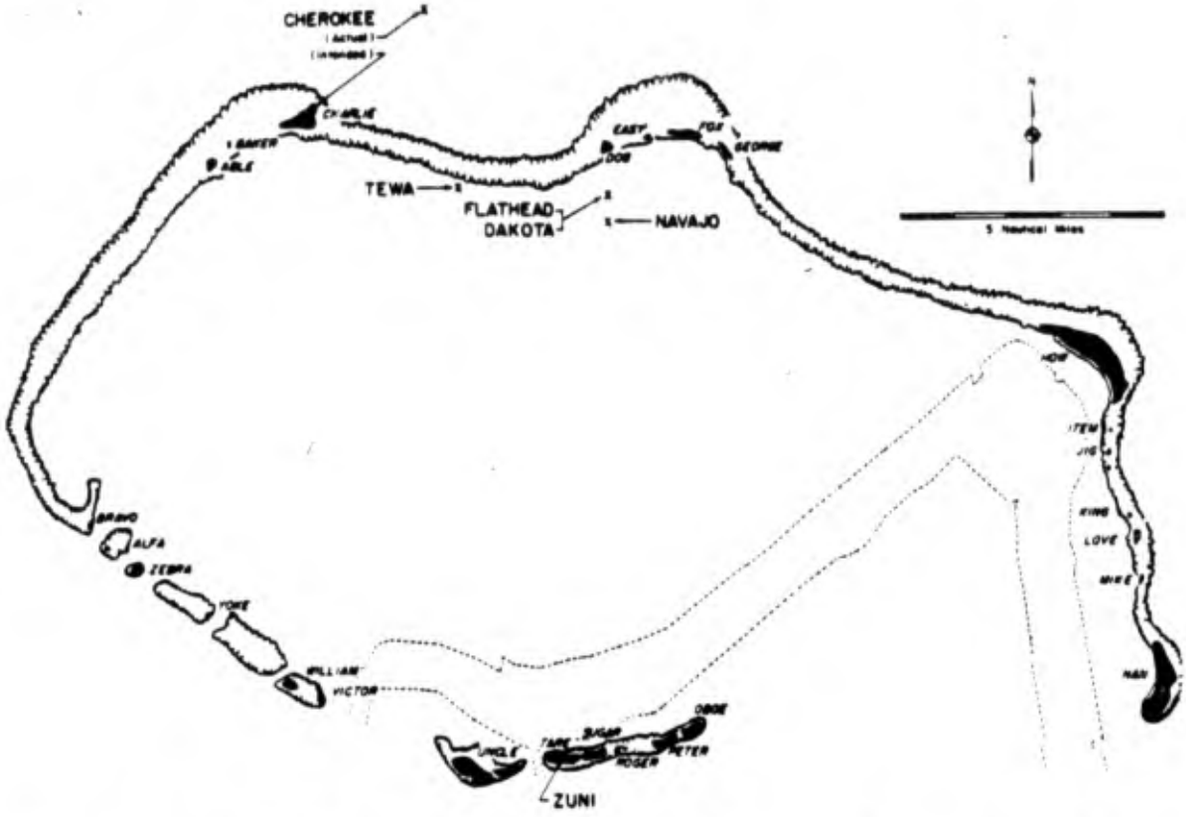

Airukiiji	Oboe	Bokoaetoktutoku	Alfa	Enitrikku	Uncle	Rochikarai	Love
Airukiraru	Peter	Bokobyaadaa	Able	Eninman	Tare	Romurikku	Fox
Aomoen	George	Bokonejien	Baker	Enyu	Nan	Rukoji	Victor
Arrilkan	Yoke	Bokonfusaku	Item	Ionchebi	Mike	Uorikku	Easy
Bigiren	Roger	Bokororyuru	Bravo	Namu	Charley	Yomyaran	Jig
Bikini	How	Chieerete	William	Ourukaen	Zebra	Yurochi	Dog
		Eniairo	King	Reere	Sugar		

Bikini Atoll. Locations of test detonations during Operation REDWING are indicated by large lettering and arrows. Native island names with corresponding military identifiers are given in the tabulation.

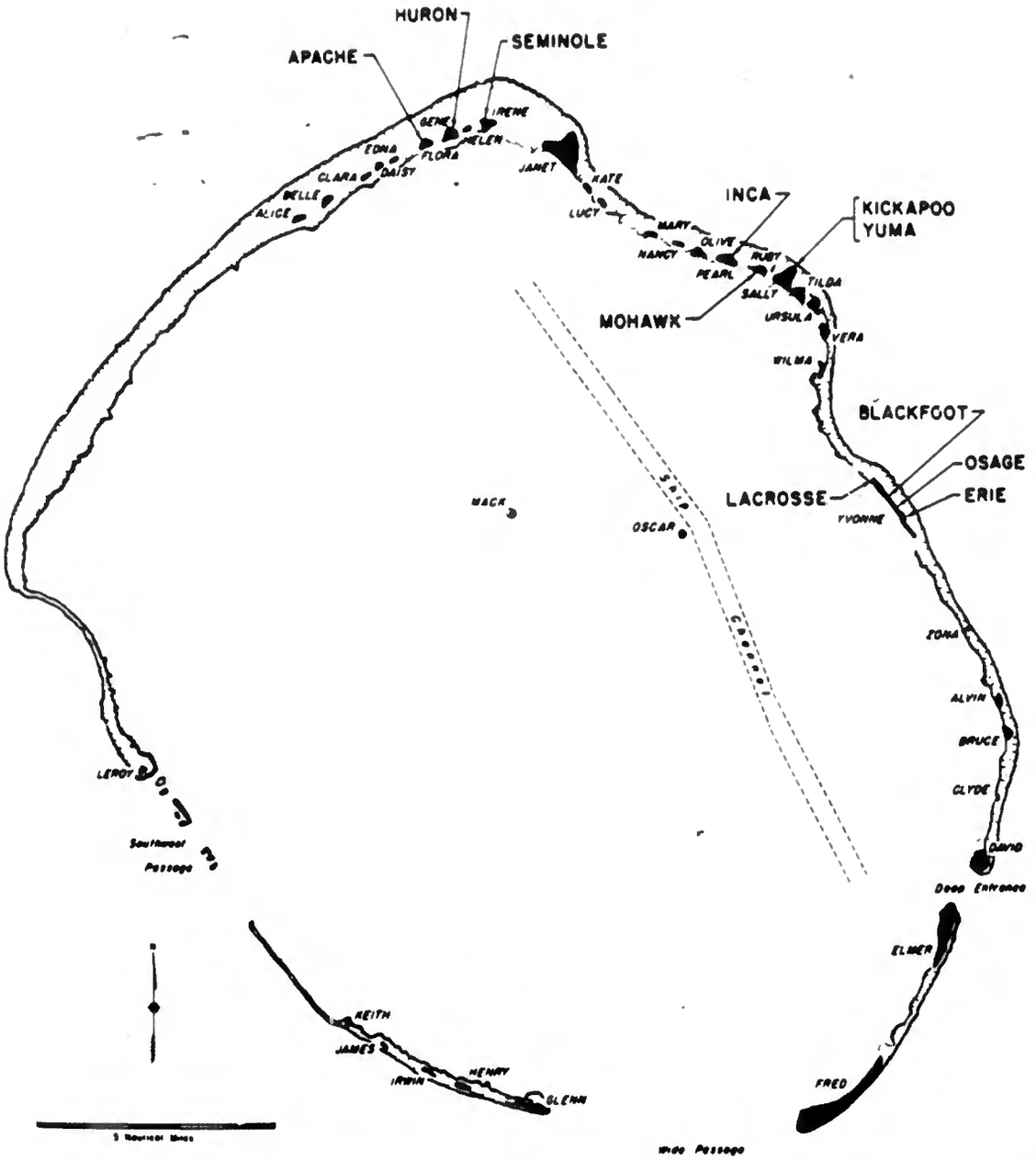

Aar uanbiru	Vera	Chinieero	Alvin	Igurin	Glenn	Ribaion	James
Aitu.	Olive	Chinimi	Clyde	Japtan	David	Rigili	Leroy
Aniyaanii	Bruce	Cochita	Daisy	Kirinian	Lucy	Rojoa	Ursula
Aomon	Sally	Coral Heads	Mack, Oscar	"M"	Zona	Ruchi	Clara
Bijjiri	Tilda	Eberiru	Ruby	Mai	Henry	Rujoru	Pearl
Bogairikk	Helen	Elvgelab	Flora	Muzia	Kate	Runit	Yvonne
Bogallua	Alice	Eng sbi	Janet	Parry	Elmer	Sandildefonso	Edna
Bogombogo	Belle	Eniwetok	Fred	Ptirsai	Wilma	Teiteiripucchi	Gene
Bogon	Irene	Girlinien	Keith	Pokon	Irwin	Yeiri	Nancy
Bokonaarappu	Mary						

Eniwetok Atoll. Locations of test detonations during Operation REDWING are indicated by large lettering and arrows. Native island names with corresponding military identifiers are given in the tabulation.

FOREWORD

This report presents the final results of one of the projects participating in the military-effect programs of Operation Redwing. Overall information about this and the other military-effect projects can be obtained from WT-1344, the "Summary Report of the Commander, Task Unit 3." This technical summary includes: (1) tables listing each detonation with its yield, type, environment, meteorological conditions, etc.; (2) maps showing shot locations; (3) discussion of results by programs; (4) summaries of objectives, procedures, results, etc., for all projects; and (5) a listing of project reports for the military-effect programs.

ABSTRACT

Project 5.4 was established to determine the response of the structure of the B-57 aircraft in flight to thermal, gust, and overpressure effects of large-yield nuclear explosions primarily for the purpose of defining the delivery capabilities of the aircraft and secondarily to obtain basic information relative to the thermoelastic response of the aircraft structure.

In order to obtain the data necessary to accomplish this objective, the aircraft was instrumented to measure the overpressure, gust, and thermal inputs, and the response of various components of the structure to these inputs. The instrumented aircraft was positioned at predetermined points in space in the vicinity of several nuclear detonations. The positions were selected such that design limits would be approached.

A maximum skin temperature of 400 F was the criterion for determination of the amount of thermal radiation which the B-57B could absorb without sustaining permanent buckling of the skin, and 600 F was the criterion for the maximum safe limit. In thermally critical participations, the aircraft was normally positioned for the 400-degrees limit for the design yield and for less than 600 degrees for the positioning yield.

With respect to gust, the aircraft was limited by 100 percent of the design limit shear at Wing Station 123. The aircraft experienced loads of from 14 to approximately 61 percent of the design limit load.

During Shot Apache, the aircraft was positioned for both overpressure and a high horizontal gust component. The results substantiated the theoretical alleviating effect of the horizontal gust component. Blast overpressures of 53 percent of the overpressure limit were received.

Sufficient data were obtained for the determination of the delivery capability of the B-57B aircraft: It was found to be better than the capability described in the B-57B Phase I-A Special Weapons Studies.

PREFACE

This report presents the final results of Project 5.4's participation in Operation Redwing. Due to the voluminous nature of the collected data, only that information necessary to support the conclusions and recommendations is presented in this report. For a complete presentation of the results of this project, the reader is referred to Wright Air Development Center Technical Note 56-465.

The technical contributions and cooperative efforts of many individuals aided in the successful completion of the objectives of the project. The authors wish to acknowledge in particular the efforts of Captain Wilbur Mitchell, pilot of the test aircraft.

The cooperation of many organizations contributed to the success of this project. The authors wish to acknowledge the efforts of those organizations including: Benson-Lehner Corporation; Radiation, Inc.; Raydist Navigation Corporation; Reeves Corporation; Wright Aeronautical Corporation; USAF Cambridge Research Center; U.S. Naval Radiological Defense Laboratory; and University of Dayton.

CONTENTS

TABLES

Chapter 1
INTRODUCTION

1.1 OBJECTIVES

Project 5.4 was established to determine the response of the structure of the B-57 aircraft in flight to the thermal, gust, and overpressure effects of large-yield nuclear explosions primarily for the purpose of defining the delivery capabilities of the aircraft and secondarily to obtain basic information relative to the thermoelastic response of the aircraft structure.

1.2 BACKGROUND

Recognizing that the delivery capability of an aircraft could be somewhat limited by its response to the induced nuclear weapon effects, the Air Force initiated a research and development program to define accurately the safe delivery capability of present-day and future aircraft. Theoretical and experimental programs conducted since 1946 (Operation Crossroads) have provided: a handbook entitled "The Effects of Atomic Weapons on Aircraft Structures"; studies of the delivery capabilities of various present-day aircraft; and substantial quantities of basic data to extend, correct, and verify the methods used to predict weapon effects.

It was necessary to participate in Operation Redwing in order to extend this program to a B-57B aircraft (Figure 1.1).

1.3 SCOPE OF INVESTIGATION

The nuclear-weapon delivery capability of the B-57B aircraft has been analytically defined in References 3 and 4. In order to confirm the criteria and methods used in this analysis or to determine if changes were required, the test program was arranged to secure the following fundamental data: (1) the relationship between weapon yield and energy inputs; (2) the temperature rise and distribution in stringers and skin panels caused by absorption of the thermal radiation; (3) the spanwise and chordwise temperature distribution as a function of thermal radiation and aerodynamic cooling; (4) the thermally induced strains in stringers and skin panels caused by thermal radiation; (5) the dynamic response of the airframe to the overpressure and gust loads; (6) the response of the engines to the thermal radiation, overpressure, and gust loads; and (7) the discovery of any aircraft components or accessories which might restrict further the delivery capability of the aircraft.

During the tests it was planned to subject the aircraft to inputs equalling or exceeding those expected under actual delivery conditions. This would provide valuable information to determine whether additional aircraft components might prove limiting as well as to demonstrate the predictability of the aircraft response up to loads to be expected in combat conditions.

1.4 THEORY AND LIMITATIONS

In order to determine the feasibility of manned operation of a B-57B weapons system in the vicinity of large-yield nuclear explosions, a study was made of the predicted response of the structure of the B-57B in flight to (1) thermal radiation, (2) overpressure of the shock wave,

(3) gust loading material velocity immediately following the shock wave, (4) gamma radiation, (5) radioactive cloud rise. The methods devised for predicting values of these phenomena are contained in References 9 and 12. The Martin Company (which had entered into contract with the Air Materiel Command [AMC] to perform the study) introduced, through References 7 and 8, some modifications of the methods outlined in References 9 and 12.

In Reference 8, the Martin Company presented a method whereby the calculated structural responses and resulting loads on the wing and tail of the B-57B airplane due to the blast effects of a nuclear explosion may be combined with the steady-state 1-g effects. This combined load can be ratioed to the design allowables to obtain variation in the amount of limit load that the

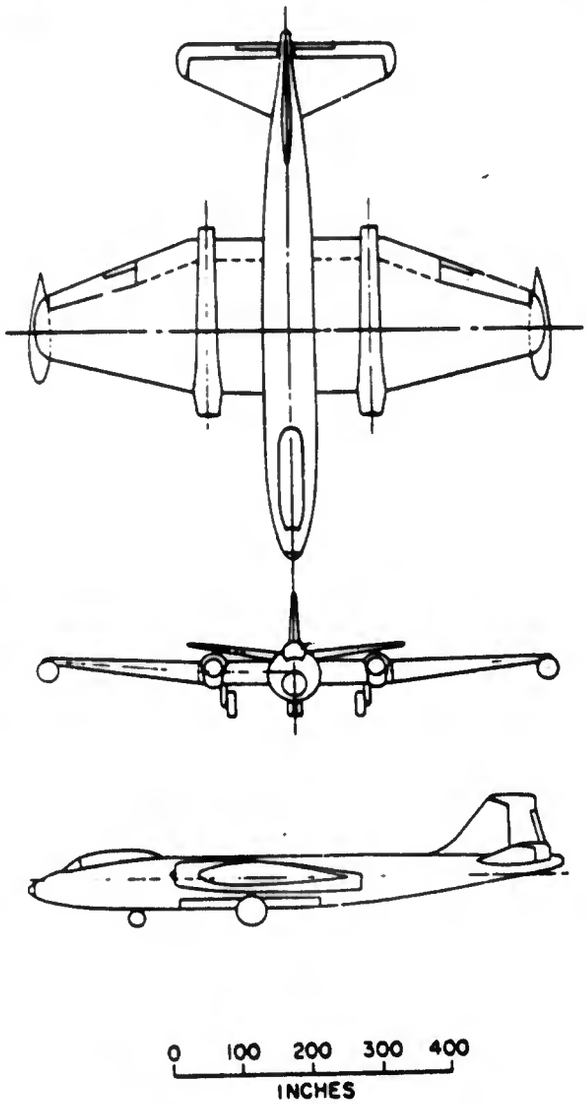

Figure 1.1 B-57B, three views.

structure sustains. One parameter may be forced through the range of expected values as the other variables are held constant and then the results may be cross plotted to obtain the evaluation of all the variables. The positioning of the aircraft due to a particular material velocity thus becomes contingent upon the cross plotting of the altitude, Mach number, time duration of the gust, and the bomb yield to obtain induced loads that are 20, 40, 60, 80, 100, and 120 percent of the design limit allowable load.

In Reference 7, a method is presented for computing skin temperature rise and allowable

thermal inputs from heating due to special weapon detonation (effects). The heat rate received by any body exposed to the detonation of a special weapon follows the general thermal pulse curve. The total amount of energy absorbed varies with the distance from the blast, atmospheric attenuation, surface absorptivity and angle of incidence of the radiation. It may be determined by an integration of the general thermal pulse curve. Thus, specific values of the heat rate will depend upon the value of the total absorbed energy and the weapon yield. Not all of the heat absorbed is available for heating the skin, since some of it is lost by convection to the aerodynamic boundary layer which is adjacent to the heated surface. In Appendix A of Reference 7, a simple method is presented based upon the heat balance equation of a unit skin area for computing skin temperatures from special weapon heating. The allowable thermal input is thus the amount of heat that may be absorbed under the thermal pulse curve to produce a maximum skin temperature rise of 400 F on the aileron tab and elevator tab.

1.4.1 Thermal Radiation Response. The allowable thermal radiation response of the B-57B aircraft was studied in detail by The Martin Company prior to the Operation Redwing field test. The investigation revealed the 0.016 skin of the aileron tabs to be the critical structural item.

The allowable thermal limits were determined on the basis of; (1) thermal loads induced in the structure which when combined with the existing loads account for changes in material properties at elevated temperatures and also (2) the residual loss of material strength associated with heating for short periods.

The structural components studied were those with 0.040 skins or thinner: minimum skin on the stabilizer (0.040), aileron (0.032), elevator (0.020), and aileron tab (0.016). The 0.051 and thicker skins on the wing and aft under fuselage were not investigated in detail since the critical thermal limit on the 0.032 skin (aileron) would cause a small temperature rise on the 0.051 skin, providing the 0.032 skin and the thicker skins have the same absorptivity.

Temperature distributions in the structure versus time were calculated for various durations of heat inputs by use of an analog computer with a method similar to that used in Reference 5. These temperatures were then entered into a thermal and airload stress analysis, and the stresses in the stringers, spars, and skin were calculated. The airloads that were combined with the thermal stresses corresponded to 1-g level-flight conditions. These stresses were then compared to the material yield strengths at the corresponding temperatures to determine the panel buckling allowables.

No loads from the gust due to special weapons were considered in combination with the thermal stresses because the gust effects occurred at the aircraft after the thermal effect and also after a time interval during which the aircraft had cooled from peak temperature to near ambient temperature.

The thinner skins on the B-57B, 24ST4 aluminum, exhibited a considerable residual loss in strength after being heated for a very short time period (Reference 6). In line with the philosophy that future use of the aircraft should not be limited by this loss of strength and that structural components should not require replacement, the maximum skin temperature was set at 400 F. The skin panels were limited to this temperature even though thermal stress requirements might allow higher temperatures.

From the above investigations it was found that the residual loss in material strength is critical for the B-57B when the skins 0.032 inch and heavier have the same absorptivity. Therefore, the all-black B-57 was limited by a midpanel temperature of 400 F on the aileron tabs, or, if the tabs were painted white, it was limited by a 400 F midpanel temperature on the 0.032-inch skins.

For positioning purposes in the Redwing tests, it was advantageous to have the maximum possible safe temperature rise. For this reason and because the aircraft was under controlled test conditions, a higher temperature limit allowing a safe degree of structural damage was investigated. From this investigation it was decided that the 0.016 aileron tabs and the 0.020 elevator tabs could be allowed to buckle and reduced material properties could be tolerated. Therefore, for this test series the maximum temperature of the tabs was set at 600 F and the

maximum temperature rise was established as 630 Fahrenheit degrees; the first of these two criteria to be fulfilled was to be the governing condition.

Thus, the thermal limits of the B-57B for the Redwing tests were set at 400 F on the 0.032-inch skin and 600 F (with a maximum temperature rise of 630 Fahrenheit degrees) on the 0.020 elevator tabs and 0.016 aileron tabs.

Since the B-57B is limited by a midpanel temperature on thin gage skin, the allowable thermal input depends only on this temperature. Therefore, to enable quick calculation of midpanel temperatures, a dimensionless curve of maximum temperature rise versus a parameter of weapon yield, convective cooling, and skin heat capacity was devised (see Reference 7). This method was used for determining skin temperatures presented in this report for comparison with the test values of the aileron and aileron tabs, the elevator and elevator tabs, and the stabilizer.

1.4.2 Overpressure. An investigation of the B-57B structure indicated that the airframe can withstand an overpressure of 2.0-psi limit (without permanent deformation) and 3.0-psi ultimate. The analysis, conducted under 1-g flight conditions, found the critical structural component for overpressure to be the aft fuselage.

A study was conducted by the Wright Aeronautical Corporation to determine the effects of overpressure on its J65W-5 engines used in the B-57B. This investigation was to determine the possibility of engine damage or flameout due to the maximum Operation Redwing anticipated overpressure of 2.0 psi. The results of this investigation showed that the engine would not be affected either operationally or structurally by overpressures up to 2.0 psi.

1.4.3 Gust Loading. The method of predicting structural loads which result from material velocity is described in Reference 8. This method assumed that the gust loads induced by the nuclear detonation impart loads similar to those induced by a normal aerodynamic gust.

Only the vertical component of the gust loading due to nuclear detonations acts on the airplane. The horizontal component affects only the relative Mach number and hence was not considered in the analysis. If the airplane were traveling away from the blast, the horizontal component of the gust load will tend to accelerate the airplane in respect to the ground, but its relative Mach number will be diminished, resulting in an alleviating effect, for the maximum loads in the airplane structure occur at some instant of time after the gust load encounters the airplane and thus at a time when the relative Mach number would already have been diminished. In the analysis each aircraft component was considered to be instantaneously enveloped by the gust.

The wing gust loads were analyzed using a three-degree-of-freedom system incorporating rigid body translation, first uncoupled symmetric bending, and first uncoupled symmetric torsion for two weight conditions: (1) 39,740-lb gross weight with 1,000 lb of fuel in each wing and (2) 37,260-lb gross weight with empty wing fuel tanks. The stabilizer was analyzed by two methods: (1) two-degree-of-freedom analysis utilizing first cantilever bending and first cantilever torsion modes and (2) two-degree-of-freedom analysis utilizing first cantilever bending and fuselage first symmetric bending modes.

The loads were determined at an altitude of 5,000 feet and a Mach number of 0.78. The altitude effects in the analysis were varied to determine altitude correction factors. Similarly, Mach number was varied to obtain Mach number correction factors. In this manner, gust loads could be predicted for altitudes between 5,000 and 45,000 feet, and Mach numbers between 0.52 and 0.78 for each of the weight conditions.

Analysis of the gust-induced structural loads on the wing, stabilizer, and aft fuselage indicated that the wing was the critical aircraft component. Use of the design limit loads (for normal flight conditions) as allowable for gust loads established a shear critical condition at Wing Station 123. The predicted stabilizer gust limitation required approximately 60 percent higher material velocity than that needed to produce the limitation on the wing.

The aircraft was limited by gust considerations on Shots Lacrosse, Erie, Inca, Blackfoot, and Huron.

1.4.4 Nuclear Radiation. The maximum permissible exposure to nuclear radiation for personnel at the test site was specified by the Commander, Task Force 7, to be 3.9 rem for any 13 week period. The nuclear radiation predicted to be received by the crew of the B-57B required consideration in only five instances in which the aircraft was scheduled to participate. Shot Kickapoo participation was withdrawn prior to the beginning of the operation. Shot Blackfoot participation was cancelled in the field, as will be explained in Chapter 3, and in the three remaining shots, the aircraft was positioned for the limiting gust loads. Nuclear radiation was not a limiting factor in any single mission. The pilot's total airborne dosage was 3.81 rem. His total airborne and ground exposure was 4.97 rem.

1.4.5 Rise of the Radioactive Cloud. In all participations the aircraft was positioned tail-on to the burst point and was flying away at time of detonation. The combination of aircraft orientation with respect to the burst point and the positions imposed by other effects eliminated cloud rise as a limiting factor. This condition would also be true in the case of an actual delivery maneuver.

1.5 INPUT COMPUTATIONS

By use of the limiting response described in the preceding section, it was desired to place the aircraft at the point in space where weapons effects would produce these responses or desired percentage of them. To locate the aircraft required the prediction of various weapon effects. Before each participation, thermal radiation, nuclear radiation, peak overpressure, and gust values in space were calculated, as described in the following paragraphs.

1.5.1 Thermal Radiation. Prediction of total thermal radiation incident on the horizontal receiver was based on the method presented in Reference 9. The Standard Eniwetok Atmosphere obtained during Operation Sandstone was used where meteorological data were required to perform the analysis. This analysis took into consideration the rise, shape, and color temperature of the fireball; the direct and reflected radiation; the atmospheric attenuation of the radiation in the visible-infrared spectrum; and the movement of the receiver during the thermal phase.

It was also desired to predict the total thermal radiation incident on a receiver normal to the slant ray between the burst point and the receiver position. These parameters were found as if the receiver were in the horizontal position by the method of Reference 9. The receiver was then rotated through an angle defined by the geometry existing between the burst point and the aircraft position. The functions of the resulting angles were then used to determine the final parameters. These new parameters were combined by the same relationship used for the horizontal receiver to obtain the total thermal radiation.

The method for computing the thermal radiation incident on a receiver at an angle other than 0 degree or 90 degrees with the slant ray between the burst point and the receiver position is described in detail in Reference 10.

1.5.2 Peak Overpressure. Peak overpressure at a point in space was calculated by using the M-problem free-air peak-overpressure curve from Reference 12 and the modified altitude correction factor (α) from Reference 18. A more detailed explanation of the M-problem method modified by the α altitude factor can be found in References 13 and 14.

1.5.3 Shock Wave Phenomena. The material velocity associated with the shock front was calculated by the method presented in Reference 12. This method equates the gust to a function of overpressure and speed of sound at altitude. The overpressure value is computed by the M-problem method modified by the α altitude correction factor as referred to in the preceding

section. The gust direction predictions were modified by using one-half the acoustic refraction correction shown in Reference 12.

The remaining phenomena (the time of shock front arrival, the peak density in the shock wave, the duration of the positive phase of the shock wave, and the triple point associated with air bursts) associated with the shock wave were computed by the methods described in Reference 12. In cases where these phenomena were dependent on functions of overpressure, the overpressures were predicted by the M-problem method modified by the α altitude correction factor.

1.5.4 Nuclear Radiation. Computation of the nuclear radiation dosage was based on the method presented in Reference 11. The method predicts the radiation received at a point in

space as the sum of the initial gamma and neutron radiations corrected for atmospheric attenuation. The B-57B was always positioned so it was flying away from the burst point. The receipt of the nuclear radiation was considered instantaneous and reduction by flyaway was neglected.

1.5.5 Cloud Growth. The growth of the radioactive cloud had not been defined analytically. Cloud growth data from previous operations were obtained from the Wright Air Development Center (WADC). These data were used to compare the aircraft positions at corresponding times after time zero with cloud position to determine if the radioactive cloud would approach the aircraft.

1.6 SELECTION OF POSITIONS

Once the aircraft response limitations had been described and the effects in space from a nuclear detonation had been predicted, a limiting position of the aircraft relative to the detonation could be defined for any particular altitude. The loci of the limiting positions over a range of altitudes formed the boundary lines of danger regions within which the aircraft must not be located. Such danger region boundaries may be combined on a feasibility diagram which indicates the aircraft limiting positions at time zero as a result of all detonation effects. Figure 1.2 presents a typical feasibility diagram.

By use of the preshot information concerning the expected capabilities of each test device, feasibility diagrams were constructed for each test in which the B-57B was scheduled to participate. Generally, these feasibility diagrams indicated that the thermal radiation and gust inputs would be the limiting effects. When possible, altitudes were chosen which would position the aircraft to receive a combination of limiting thermal radiation and limiting gust inputs. Where combined limits could not be received, a compromise position was chosen to receive effects which the preshot information indicated would provide the most valuable data. In this way, the desired preliminary positions were evolved.

Generally, instead of the desired combined limiting effects, the aircraft position was limited by only one effect at a time, either thermal radiation or gust. Thermal limiting positions were based on the no-structural-damage limit referred to in Section 1.4.1 and were the limiting criteria on Shots Zuni Gust limiting positions were based on 95 percent of the limit allowable load resulting from gust and were the limiting criteria on Shots

Some exceptions were made to the general positioning criteria referred to immediately above.

For Shots Lacrosse aircraft was positioned for 80 percent of limiting effects. These shots were the first two of the series, and the reduced limits were imposed to guarantee aircraft safety until positioning methods were confirmed. The results obtained were then used as guides to positioning the aircraft for succeeding participations. All other exceptions were based on positioning the aircraft to exceed the no-damage limits in order to confirm the no-damage limit criteria. Additional comments on the exceptions to the general positioning criteria are presented in Chapter 3.

The yields used for devising the feasibility diagrams were design and positioning yields. The positioning yield was used to determine the aircraft position to obtain the desired weapon effects.

Chapter 2
PROCEDURE

With the requirement established for the B-57B aircraft to participate in Operation Redwing, The Martin Company was contracted by the Air Materiel Command (AMC) to assist the Wright Air Development Center (WADC) in planning and conducting the tests.

A production version of the B-57B was selected to be instrumented while the particular aircraft (B-57B S/N AF 52-1569) was still in the production line of The Martin Company. The engineering for the installation of the instrumentation was started in January 1955, and the instrumented aircraft was delivered to contractor flight test in October 1955. In March 1956, the aircraft was flown to the Pacific Proving Ground by WADC personnel.

In addition to the installation of the instrumentation, The Martin Company performed the calibration, maintenance, and operation of the instrumentation and its associated equipment; the development of positions and positioning methods; and the reduction and correlation of data. The test aircraft, itself, was flown and maintained during the operation by WADC, Directorate of Flight and All Weather Testing. The general organization under which this project operated is shown in Figure 2.1.

2.1 OPERATIONS SCHEDULE

The original operations plan for this project was conceived during the summer and fall of 1955, as preliminary knowledge was obtained concerning the expected yields for the various devices to be detonated during the operation. All detonations with the exception of Shots were scheduled for participation. They are arranged in Table 2.1 in chronological order together with their dates, height of burst, and design and positioning yields.

2.2 POSITIONING

A meeting of positioning representatives for all aircraft was held and all desired positions were discussed. Conflicting altitude choices were resolved and incremental changes in altitudes were made when required to ensure safe separation of all test aircraft. The resulting altitudes became the assigned test altitudes, and final positions were obtained from the feasibility diagrams.

The MSQ-1A/APW-11A system was used to position the aircraft for detonations at Eniwetok Atoll. An electronic system devised and operated by the Raydist Navigation Corporation, under contract to WADC, was used to position the aircraft for detonations at Bikini Atoll. Tracking information from the MSQ-1A/APW-11A system was recorded by the addition of a radar data box to the MSQ-1A unit. Tracking is an automatic function of the Raydist system.

2.2.1 MSQ-1A/APW-11A System. The MSQ-1A/APW-11A close support radar unit was used to position the aircraft for the following detonations: Lacrosse, The aircraft was equipped with an AN/APW-11A radar beacon system as standard equipment. This beacon transponder permits the MSQ-1A system to maintain a positive electronic contact with the aircraft. Timing signals from the firing bunker on Elmer Island were transmitted to the MSQ-1A control van to furnish an accurate visual indication on the aircraft tracking record of certain times relative to H-hour. The MSQ-1A tracking information was photographically recorded in the radar data box trailer.

Generally, the aircraft takeoff time was at H−48 minutes. Immediately after takeoff, the aircraft was under the control of the Air Operations Center (AOC). As soon as the MSQ-1A system established positive contact, the control was passed to the MSQ controller with the AOC acting as monitor. By UHF radio contact the controller advised the pilot of the aircraft's relative timing error and directed the aircraft to the time zero position.

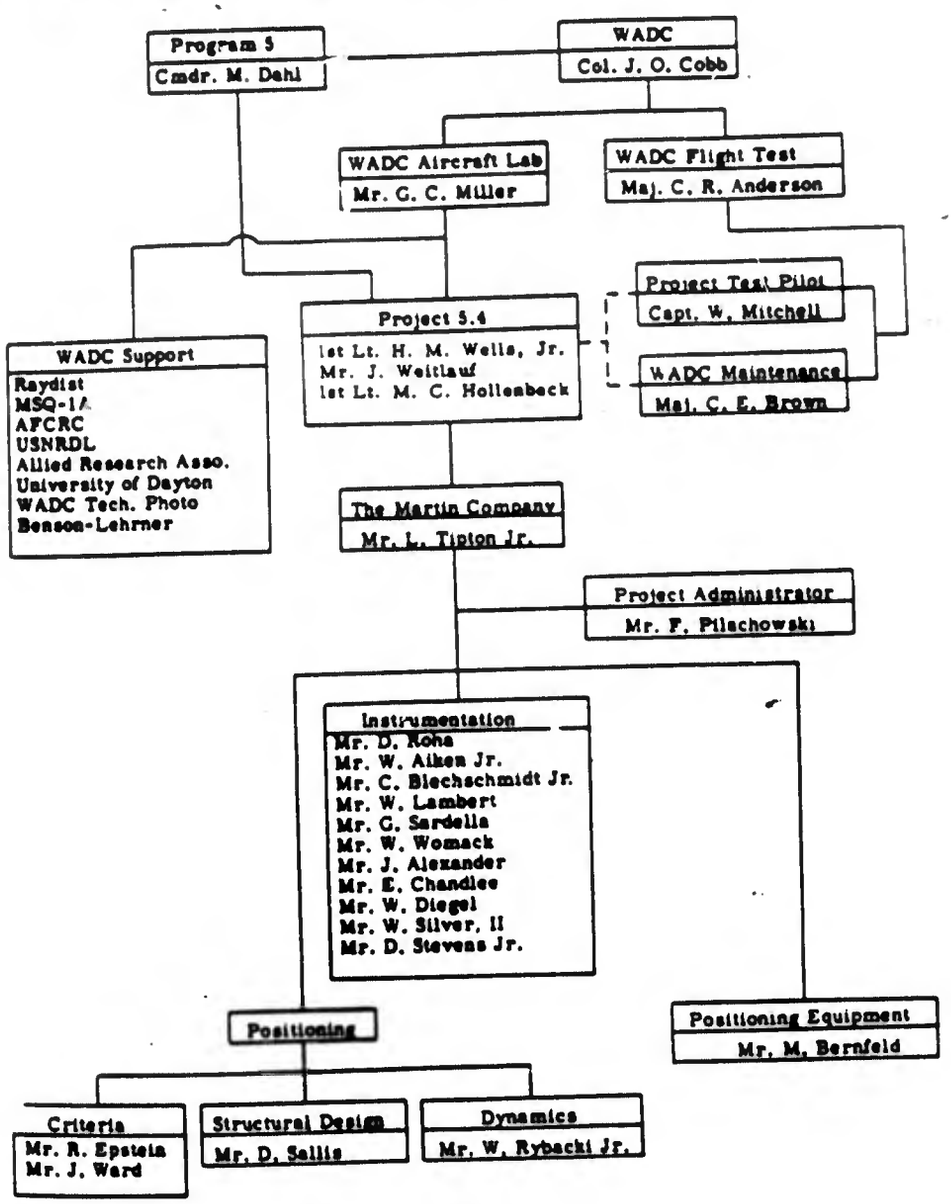

Figure 2.1 Organization chart.

2.2.2 Raydist System. The Raydist system consisted of four relay stations on How, Nan, William, and Fred Islands, a reference station on Wotho Island, a master station on the USS Badoeng Strait, and the aircraft's airborne station. The tracking system was arranged to give simultaneous position information to the ground controller and to the pilot.

The airborne equipment consisted of a 100-watt low-frequency radio transmitter, an antenna loading unit, a power dynamotor, a demodulator, an external wire antenna, an IL 525 course

indication unit, an ARC-3 VHF radio receiver, and a whip antenna. The IL 525 unit was installed in the pilot's main control panel. The wire antenna was installed in a V-shape between the vertical fin and a point on each wing above the main landing gear well. The whip antenna was installed on the under surface of the left wing immediately behind the main landing gear well. All other equipment was installed in the aft fuselage.

Utilization of the Raydist system originally required a flight at the test altitude and speed prior to each event during which a tape recording was made of the signals from the Raydist transmitter and receiver complex. The tape was then edited to place the aircraft at its proper spot fifteen minutes from the time zero position of the actual mission. During the tape cutting and the actual missions the aircraft was kept in the proper azimuth lane by telemetering azimuth signals from Nan and How stations. Early in the operation, a method of simulating mission recordings was devised and the tape-cutting mission was deleted. During an actual mission the signals from the Raydist transmitter were compared to the signals on the tape. The timing distance error was telemetered to the aircraft by VHF and was presented to the pilot as a visual display of progress and azimuth. In addition, the ground controller on the USS Badoeng Strait advised the pilot of the progress and azimuth errors by UHF radio. The Raydist ground controller could voice-control the aircraft in the same manner as the MSQ-1A system controller in the event the pilot's visual equipment failed.

A typical flight to Bikini Atoll for test participation would begin with takeoff at H−45 minutes. AOC controlled the aircraft until the MSQ-1A controller had positive radar contact. The MSQ controller then assumed control and directed the aircraft to cross the Fred-Nan progress line ten miles west of Fred Island, thence to a predetermined point eighteen minutes flying time from the time-zero position. Upon arrival at this point, the Raydist controller assumed control and began to telemeter azimuth information. At H−15 minutes, an electrical signal from the firing bunker on How Island initiated the progress tape, and the Raydist controller started telemetering progress information. After the detonation, the Raydist controller directed the aircraft to cross the How-Nan azimuth line south of Nan Island to provide a second reference point for the Raydist tracking calculations. While under Raydist control, the aircraft was being monitored by the Combat Information Center (CIC) aboard the USS Estes. The return flight to Fred Island was controlled by this CIC to a point 90 miles from Fred Island where AOC again assumed control.

2.3 FLIGHT PATTERNS

Upon the resolution of any position conflicts, final positions were available for each aircraft; flight patterns were then devised for each event. These patterns contained all the pertinent data on aircraft positions, desired courses, scheduled times the aircraft should be at various locations, the controllers and times they would assume control, and necessary abort data. The flight patterns were distributed to the crew of the aircraft, to the controllers, the monitors, and other interested personnel prior to each event. Typical flight patterns are presented in Figures 2.2 and 2.3.

2.4 RECORDING EQUIPMENT

The time-history data were recorded on five 50-channel Consolidated Electrodynamic Corporation (CEC) oscillographs (Type 5-119-P3). Each oscillograph recorded a self-generated

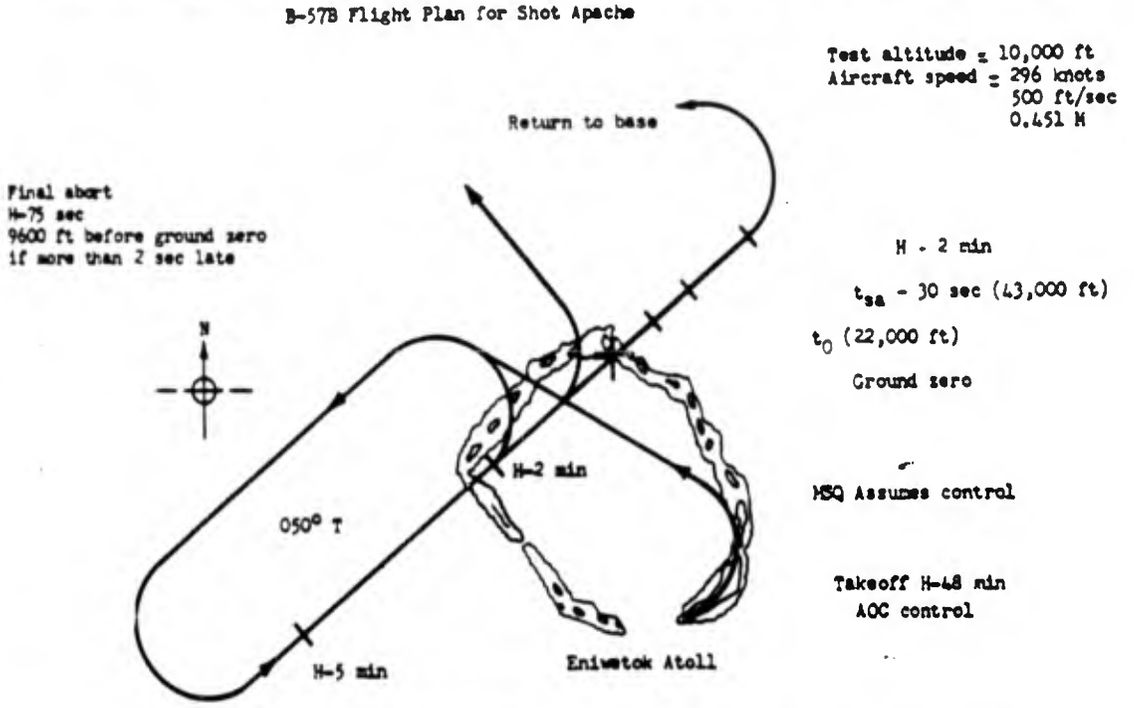

NOTES: 1. H-5 min and H-2 min are check points used by Commander TG7.4 to ensure that the aircraft is in a position within its ability to make up any tardiness.

2. Aircraft climbs to test altitude immediately after takeoff.

3. Three complete race tracks are flown.

Figure 2.2 Typical MSQ flight pattern.

100-cps time base as well as a synchronizing pulse from a common external source. The instrument model numbers and the frequency response of each recording system are shown in Table 2.2.

The auxiliary equipment utilized in the recording system can be divided into five main types: (1) bridge balance units, (2) bridge calibration units, (3) thermocouple calibration units, (4) channel attenuating and damping units, and (5) the master control units. A channel in the bridge balance unit was required for each strain, pressure, acceleration, and position measurement. A calibration channel was utilized for each of the preceding measurements in order to accomplish an automatic in-flight electrical calibration. The thermocouple calibration unit impressed a known voltage source in each thermocouple, calorimeter, and radiometer channel. Each recording channel utilized an attenuating unit which permitted the adjustment of the measurement

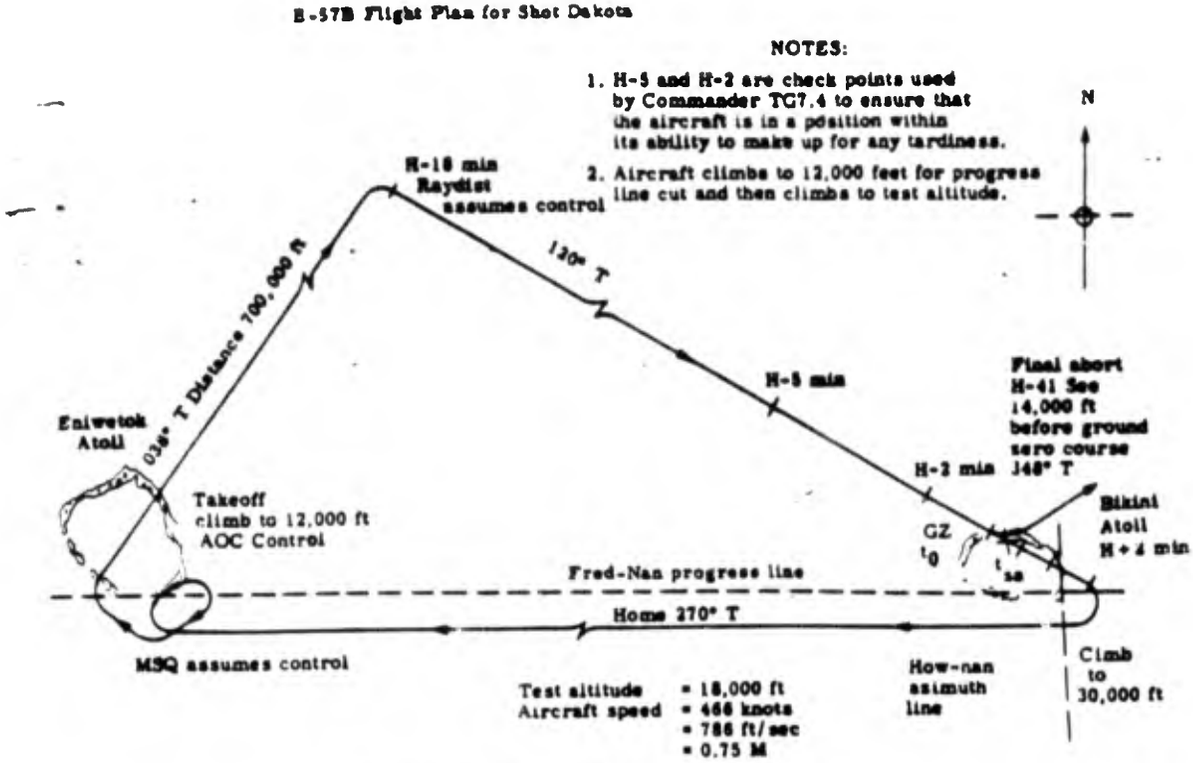

Figure 2.3 Typical Raydist Flight Pattern

TABLE 2.2 INSTRUMENT TYPES AND RESPONSE

Instrument	Manufacturer	Model	System Frequency Response
Accelerometer	Statham Laboratories	A5A-5-335	20 cps
	Statham Laboratories	A5A-15-335	20 cps
	Statham Laboratories	AA19-15-300	12 cps
	Statham Laboratories	AA19-8-300	6 cps
Airspeed	Giannini	E835028-3	Limited by standard pitot installati
Altimeter	Giannini	E835027	Limited by standard pitot installati
Outside Air Temperature	Giannini	4915E	—
Vertical Gyro	Giannini	3111N	—
Directional Gyro	Giannini	3211N	—
Overpressure	Statham Laboratories	P96-20 D-350	60 cps
	Statham Laboratories	P69-1D-350	60 cps
	Statham Laboratories	P69-3D-350	60 cps
Engine Pressure	Consolidated Electrodynamic Corp	4-312-5 PS 1D	60 cps
	Consolidated Electrodynamic Corp	4-311-50G	60 cps
	Consolidated Electrodynamic Corp	4-313-250A	60 cps
	Consolidated Electrodynamic Corp	4-312-50A	60 cps
Magnetic Heading	Gyro Compass	JU-2	—
Radiometer	NRDL	—	—
Calorimeter	NRDL	—	—
Surface Position	Allen Bradley	JU 5000	60 cps
Strain Gages, gust load	Baldwin-Lima	EBDF-13D	60 cps
Strain Gages, thermal	Baldwin-Lima	EBD-1D	60 cps
Temp-Tape	University of Dayton	--	—

sensitivity and a damping unit which allowed each channel to be adjusted for the desired flat-frequency-response range. The master control box directed the oscillograph paper speed, automatically started cameras and changed paper speed at the prescribed times, and controlled the automatic calibration and zeroing functions of the various units.

2.5 THERMAL INPUT INSTRUMENTATION

The measurement of thermal inputs can be divided into three categories: (1) radiant exposure, (2) irradiance, and (3) fireball spectral analysis.

2.5.1 Radiant Exposure. Total radiant exposure was measured with calorimeters furnished by United States Radiological Defense Laboratory (USNRDL) to fulfill data requirements set by

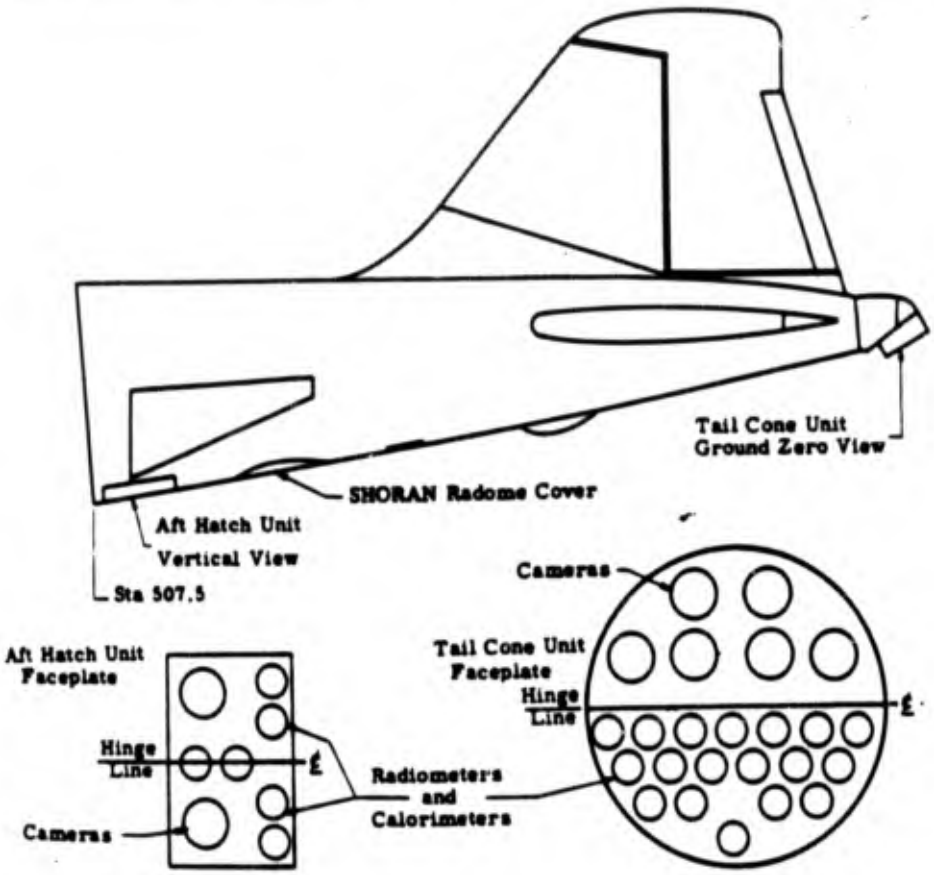

Figure 2.4 Thermal input instrument locations.

Project 5.7 (USAF Cambridge Research Center). Calorimeters were located in the tail cone (oriented toward ground zero), the aft hatch (oriented in the vertical plane), and inside the Shoran radome. Calorimeter instrument locations are indicated in Figure 2.4. The desired calorimeter system sensitivity was obtained by selection of the proper galvanometer and attenuating resistance combination. The system was electrically calibrated before each flight by application of known voltage source increments.

2.5.2 Irradiance. Irradiance was measured by radiometers which were located in the tail cone and oriented toward ground zero. Radiometer locations are indicated in Figure 2.4. The sensitivity adjustments and calibration procedures of the radiometer were similar to those of the calorimeter system.

2.5.3 Fireball Spectral Data. Fireball spectral data including spectral analysis of the fireball, albedo effects, and the angular relationship of the aircraft to the fireball were recorded by type N-9 gun cameras (Bell and Howell). Six cameras were located in a special tail cone oriented toward ground zero and two cameras were mounted in the bottom aft fuselage hatch and oriented vertically toward the ground (Figure 2.1). The camera units in the tail cone were adjusted on the ground prior to each test. The lenses and filter combinations which were utilize in the various tests are noted in Table 2.3.

2.6 GUST INPUT INSTRUMENTATION

Overpressure measurements were made at seven locations on the aircraft, as indicated in Figure 2.5. The pressure transducers were calibrated by applying known static pressure with a U-tube containing mercury. The ambient pressure side of the transducer was sealed at test altitude immediately prior to time zero through activation of a solenoid-operated valve. The pressure pickup tubing and recording equipment were chosen to provide a flat-frequency response to 60 cps.

TABLE 2.3 CAMERA LOCATIONS AND FILTERS

B + W = Black and White; Doc = Documentary

Detonation Code	Position 1	Position 2	Position 3	Position 4	Position 5	Position 6	Position 7	Position 8
Lacrosse	B + W, Doc	color Doc	red filter	spectrographic	spectrographic	blue filter	yellow filter	yellow filter
Zuni								
Erie								
Flathead								
Inca								
Dakota								
Apache								
Huron				red filter	blue filter			

2.7 THERMAL RESPONSE INSTRUMENTATION

2.7.1 Temperature Measurements. Time-history temperature measurements were made on the skin and stringers of the stabilizer, elevator, elevator tab, aileron, and aileron tab. The iron-constantan thermocouples were located to produce temperature surveys of typical stringers and skin panels, as shown in Figures 2.6, 2.7, and 2.8. Duplicate thermocouples were installed for each measurement on the stabilizer, elevator, and aileron. A reference junction was maintained at 32 F for each thermocouple channel. The thermocouple channels were electrically calibrated by applying known millivolt-source increments to the system before each flight. The relationship between temperature and millivolts was obtained from National Bureau of Standards, Circular 561 "Reference Tables for Thermocouples". The reference point (32 F) was established by the automatic calibration at the end of the detonation record.

Peak temperature measurements also were made with Temp-Tape on the skin at various places on the control surfaces: flaps, wing, stabilizer, and fuselage. The Temp-Tapes, produced by the University of Dayton, are 1¼-inch by 2-inch rectangles of Scotch brand tape to which twenty ⅛-inch pigmented circles are attached (Reference 15). Each pigmented circle melts at a particular temperature. The melting of one or more pigments affords the information regarding the range of the peak temperature experienced by the surface to which the tape has been applied.

The University of Dayton furnished the calibration data for the Temp-Tapes. The melting points of the pigmented circles are separated by approximately 20 Fahrenheit degrees. Care

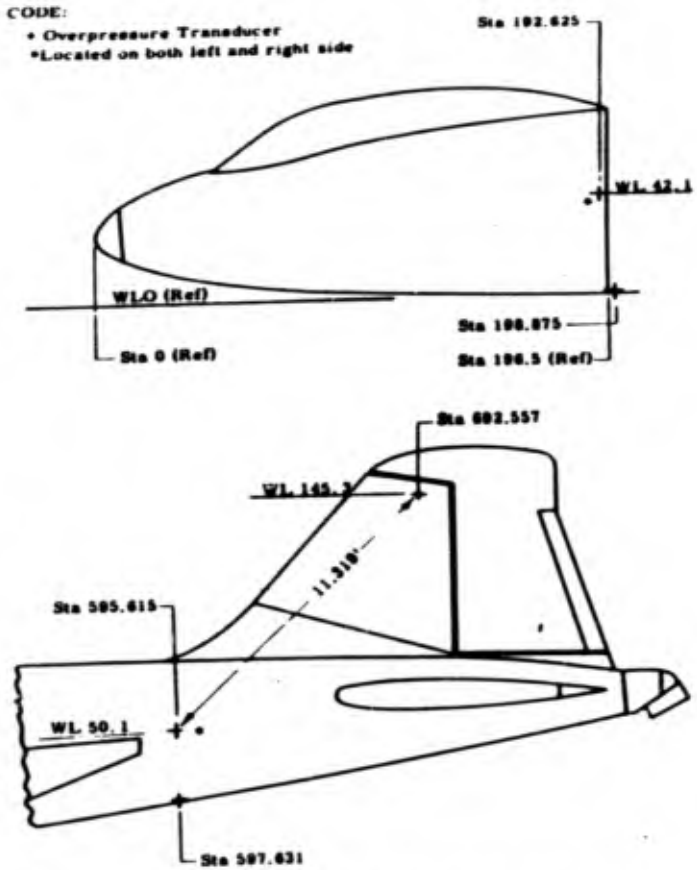

Figure 2.5 Overpressure transducer locations.

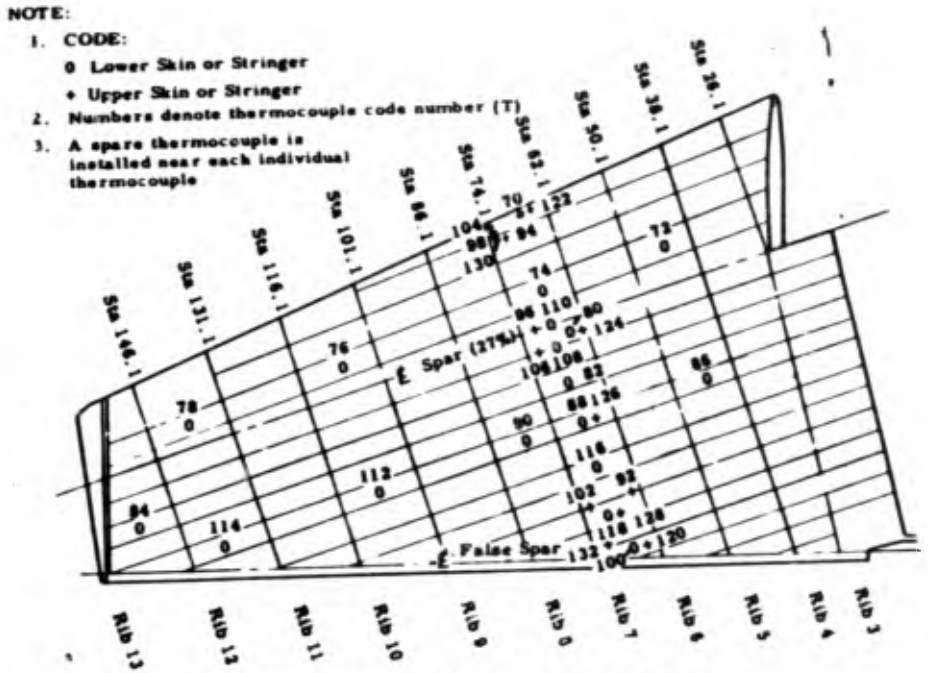

Figure 2.6 Thermocouple locations, left stabilizer.

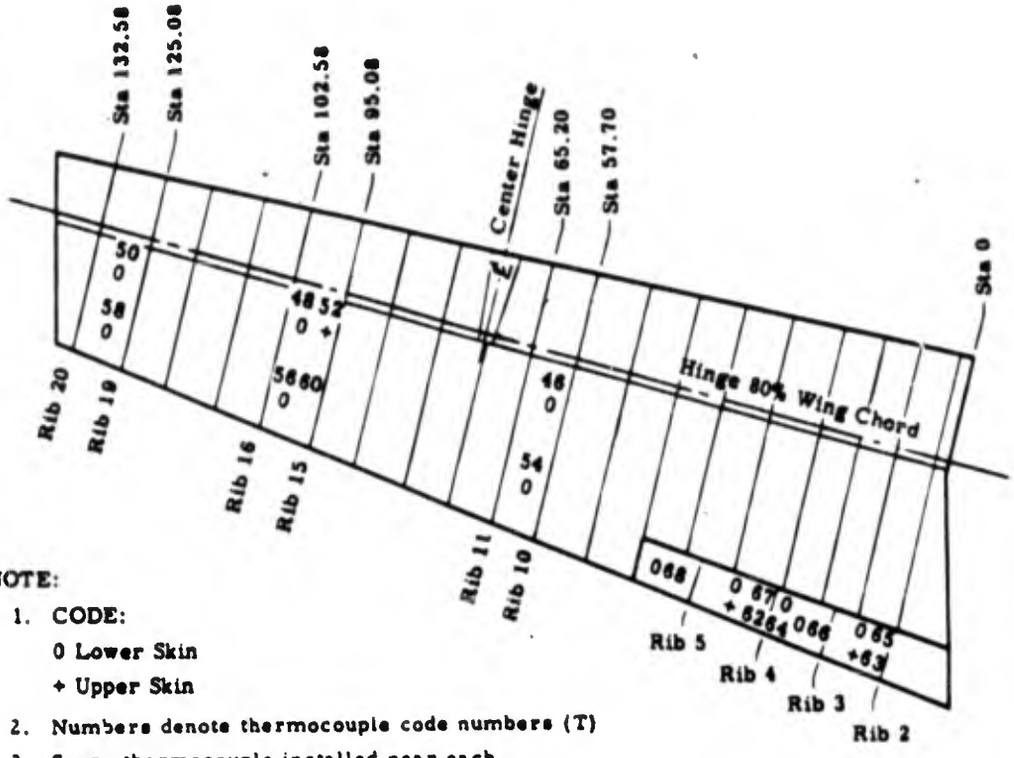

NOTE:

1. CODE:
   0 Lower Skin
   + Upper Skin
2. Numbers denote thermocouple code numbers (T)
3. Spare thermocouple installed near each individual thermocouple

Figure 2.7 Thermocouple locations, left aileron and aileron tab.

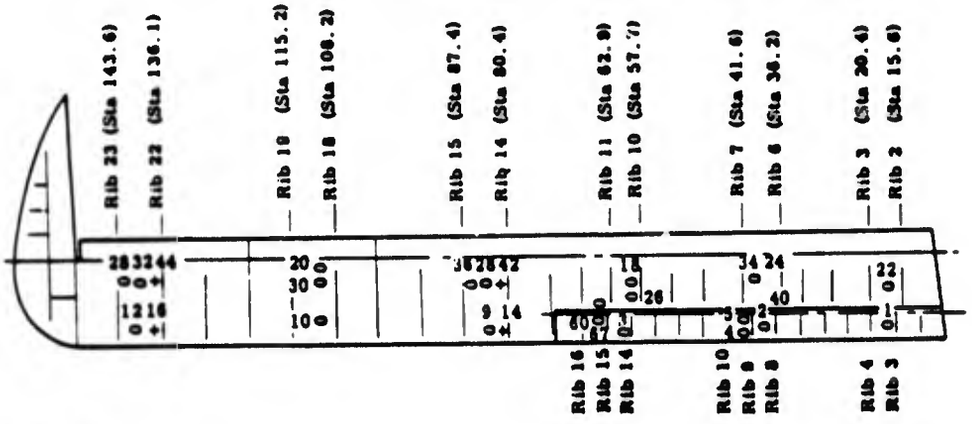

NOTES:

1. CODE:
   0 Lower Skin
   + Upper Skin
2. Numbers denote thermocouple code number (T)
3. Spare thermocouple installed near each individual thermocouple

Figure 2.8 Thermocouple locations, left elevator and elevator tab.

must be exercised in the interpretation of the data since the pigments are affected by sun-induced skin temperatures, moisture, hydraulic fluid, and age. Generally, several Temp-Tape installations on similar structure should be made in order to obtain reliable data.

2.7.2 Thermal Stress. Thermally-induced stress on the stabilizer skin and stringers was measured by strain gages (Baldwin Type EBD-1D) installed between ribs 6 and 7. Each strain-gage bridge consisted of one active gage located on the skin or stringer and three dummy gages installed on an aluminum panel which was mounted on a rubber pad inside the stabilizer. The locations of the active gages are shown in Figure 2.9. The gage factor furnished by the gage manufacturer was used in an empirical formula to obtain the calibration. The electrical sensitivity of the strain-gage system was automatically calibrated at the end of the detonation record. The thermal strain was taken as the change in strain level from that which existed immediately prior to detonation time zero (T_0).

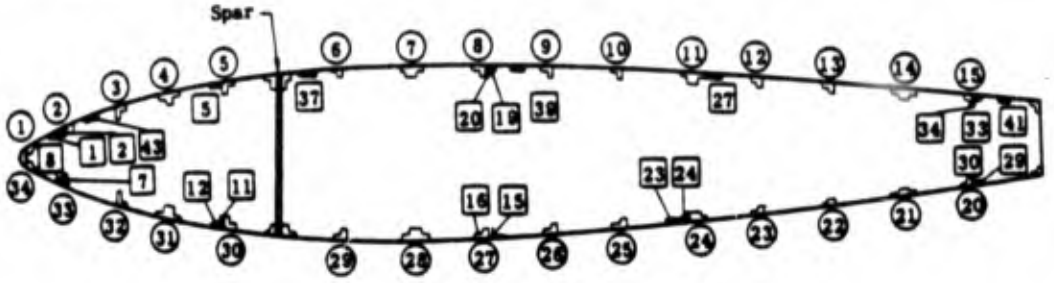

NOTE:

1. CODE:
   - Thermal Strain Gage (Code BH)
   - Stringers
2. Spare strain gage installed near each individual strain gage
3. Compensating gages were glued to pads which were on outboard face of Rib 6, Sta 62.1 and inboard face of Rib 7, Sta 74.1

Figure 2.9 Thermal strain gage locations, left stabilizer.

2.7.3 Surface Position. Surface positions were measured by means of precision potentiometers mounted to indicate stabilizer incident angle, left elevator position, left elevator-tab position, and left aileron position. Calibration was accomplished by establishing known angular positions with templates and recording the output of the displacement bridge at each position. The bridge system electrical sensitivity was calibrated at the end of the detonation record.

2.7.4 Angular Measurements. Flight-attitude, angles of roll, pitch, and yaw were measured with directional gyros located at Fuselage Station 550. The gyros were caged on the ground and were uncaged on the final approach before time zero. The gyros were calibrated on a swivel table at the Martin facility prior to departure to the forward area. The gyros were electrically calibrated at the end of each detonation record. The change in the angular position of the aircraft from straight and level flight was measured.

2.7.5 Airspeed and Altitude Measurement. Airspeed and altitude were recorded by means of the standard B-57B pilot installation. The pressure pickups were calibrated by applying known static pressures with a T Tube using mercury. The indicated airspeed and altitude were corrected for position error. The corrected altitude then was compared with the weather balloon pressure-gradient data to obtain absolute altitude.

2.8 GUST RESPONSE INSTRUMENTATION

2.8.1 Accelerations. Accelerations were measured with accelerometers which determined the rigid body translation and dynamic response of the aircraft. The locations of the accelerometers are indicated in Figure 2.10. Linear accelerometers were located at five stations along the left wing, in the right wing tip, at four stations along the fuselage, and at each stabilizer tip. The accelerometers were calibrated with an electrodynamic vibrator prior to departure to the forward area. A 2-g calibration was accomplished periodically during the operation. Angular accelerometers were located at the aircraft center of gravity to sense accelerations about the pitch and roll axes. The angular accelerometers were calibrated on a swinging pend-

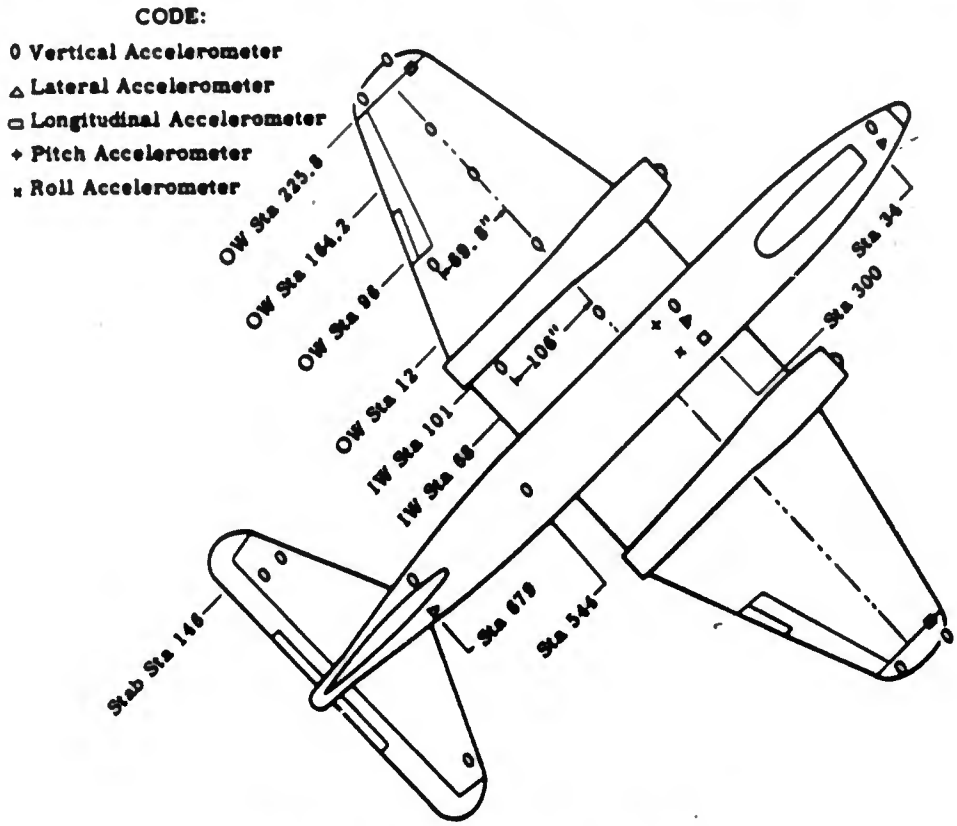

Figure 2.10 Accelerometer locations.

ulum at the Martin facility. All accelerometer channels were calibrated electrically at the end of each detonation record. The accelerometer system was overdamped electrically to provide a flat-frequency response to approximately 20 cps. In this manner, the higher dynamic acceleration responses were filtered.

2.8.2 Structural Loads. Structural loads were measured by strain gages installed on the wing, stabilizer, and aft fuselage. Each bridge consisted of four active-strain gages (Baldwin EBDF-13D temperature compensated strain gages). The bridges were calibrated by the point loads method (Reference 16) and electrically combined into networks to measure shear, moment, and torque. The strain gage networks were located at three stations on the left wing, one station on the right wing, one station on each stabilizer, and two stations on the aft fuselage. Locations of the wing bridges are indicated in Figure 2.11, and the stabilizer bridge locations are shown in Figure 2.12. Single bridge networks were located at Fuselage Stations 595 and 472. The point-loads static calibration was followed by an in-flight calibration program conducted at the Martin facility in January 1956 (see Reference 17). These data were utilized to determine

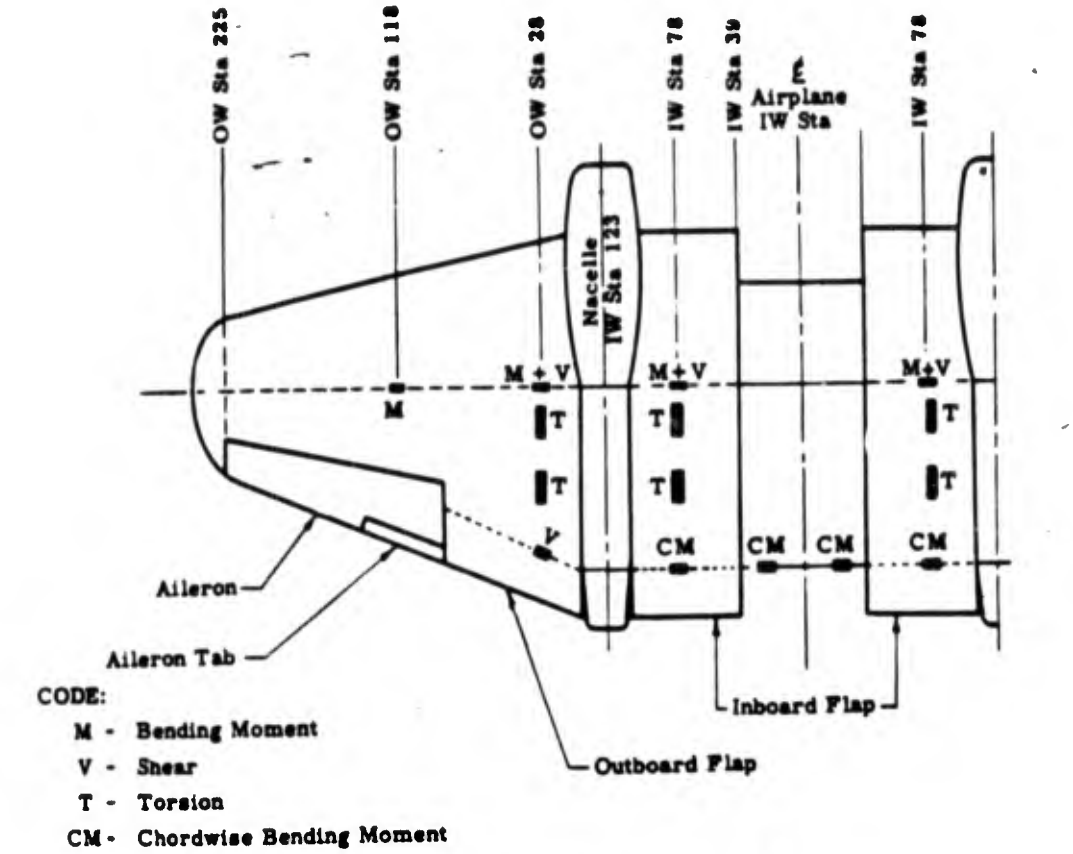

Figure 2.11 Airload bridge locations, wing.

NOTES:

1. CODE:
   - M - Bending Moment
   - V - Shear
   - T - Torsion
2. Airload bridges located on both left (shown) and right side of stabilizer

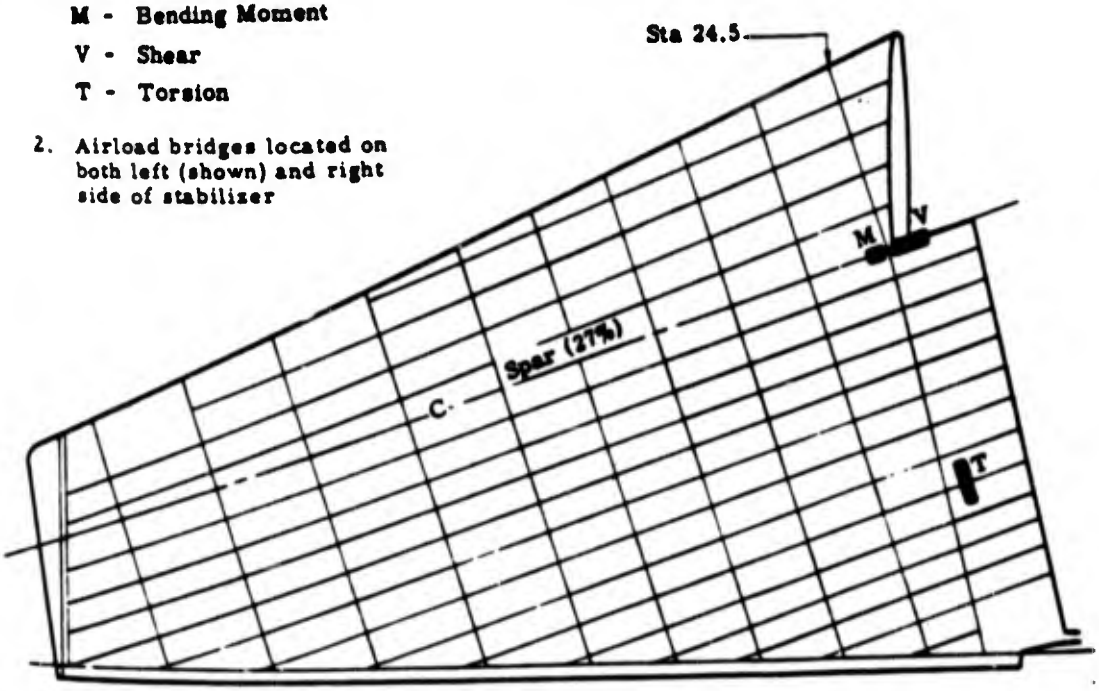

Figure 2.12 Airload bridge locations, stabilizer.

the structural loads during straight and level flight (1-g flight condition). The gust load bridges were electrically calibrated on each detonation record. The calibrations of the primary bridges were checked in the forward area by the application of loads.

2.8.3 Power Plant Measurements. Power plant measurements included: (1) a pressure survey along two compressor inlet struts; (2) compressor discharge total and static pressures, and turbine outlet total pressure; (3) compressor inlet and tailpipe temperatures; (4) engine speed; (5) fuel flow; and (6) temperature and differential pressure in the fuel vents of the left

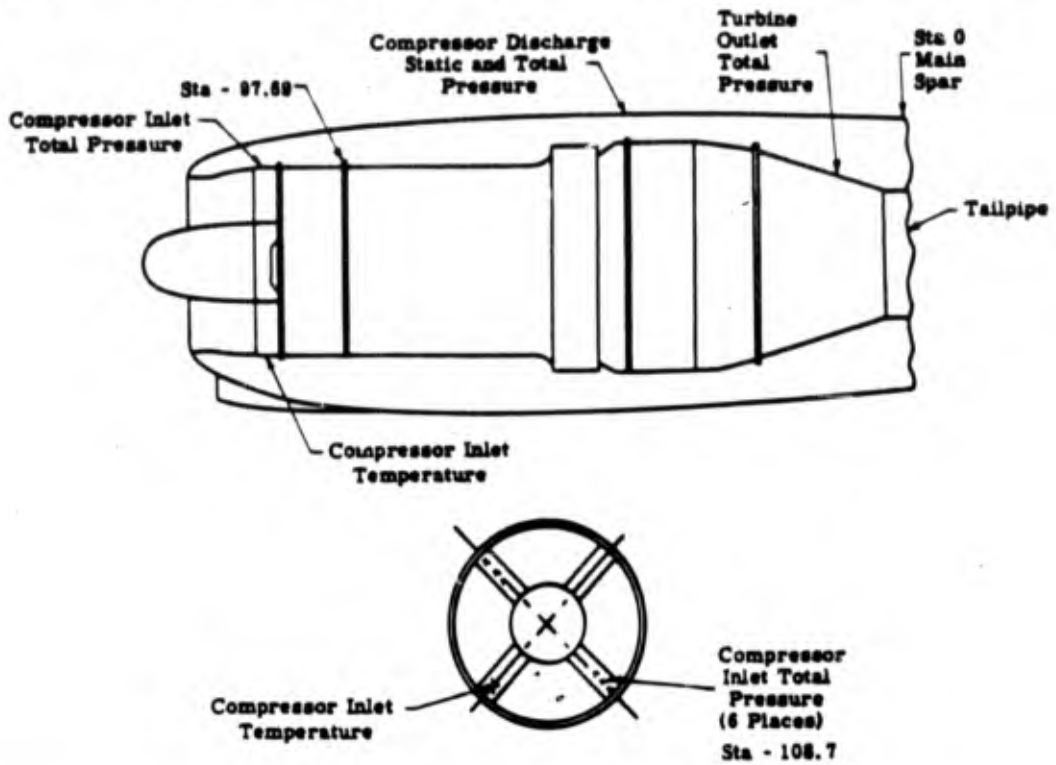

Figure 2.13 Right engine instrument locations.

wing and number two fuselage tanks. Power plant instrumentation locations are shown in Figur 2.13. The pressure pickups were calibrated at the contractor's facility with a manometer. The pressure system was calibrated electrically after each detonation record. The standard tail pipe temperature and tachometer installations were utilized.

2.9 NUCLEAR RADIATION INSTRUMENTATION

Nuclear radiation received was obtained from film badge dosimeters worn by the pilot and observer during each detonation.

Chapter 3
RESULTS

The data obtained by the B-57B participations in Operation Redwing were recorded on oscillograph records and motion picture film. The recorded data represented the primary results of Project 5.4. The records were then carefully reduced and analyzed. The reduced data are presented in Reference 2. General flight data and the average final peak values of inputs and response for each event in which the B-57B successfully participated are presented in Tables 3.1 to 3.8. Pertinent meteorological conditions at detonation times are presented in Table 3.9. Time histories of significant inputs and responses are presented in Figures 3.1 through 3.6.

3.1 SHOT LACROSSE

The B-57B aircraft participated successfully, and good data recordings were obtained. No visible damage to the aircraft resulted from this shot. The aircraft was positioned for 80 percent of the limiting gust load. The preliminary data recorded were used as a guide for positioning the aircraft in succeeding events.

3.2 SHOT CHEROKEE

This mission was aborted prior to time zero due to malfunctioning of the Raydist positioning system.

3.3 SHOT ZUNI

The B-57B participated and obtained good data recordings concerning the thermal effects and responses. However, no data concerning the blast effects or responses were recorded because the recording equipment was inadvertently turned off prior to the arrival of the shock front. The aircraft was guided by the Raydist positioning system to the desired time zero position. The aircraft was positioned for the no-structural-damage thermal limit, that is, a maximum temperature of 400 F on the aileron tabs.

Some visible damage resulted from this test. The paint was scorched on the aileron tabs and the marker beacon radome. The pilot obtained the sensation that the shock effects from this detonation were greater than the effects from Shot Lacrosse. However, with no blast data recorded, this impression could not be confirmed. The actual gross weight of the aircraft at time of shock front arrival was very nearly equivalent to the predicted condition. Preliminary data from this shot in conjunction with the thermal data obtained in Shot Lacrosse were used as a guide for positioning the aircraft for subsequent thermal limiting participations.

3.4 SHOT ERIE

The aircraft participated successfully, and good data recordings were obtained. Satisfactory positioning of the aircraft was attained by the MSQ-1A positioning system. No visible damage to the aircraft resulted from this test; however, one effect at time of shock arrival is worth noting. Garbled messages were transmitted through the microphones in the aircraft while the aircraft was receiving the blast effects; it is believed that this interference was caused by the passage of the shock front. With the aircraft on an outboard reading from ground zero at time zero, it is desirable for the computed values of t_{max} to be less than the measured values. The aircraft was positioned for the limiting gust loads for this event.

TABLE 3.1 DESIRED AND ACTUAL AIRCRAFT LOCATIONS, IN FEET

Shot	Horizontal Range at Time Zero		Altitude at Time Zero		Offset at Time Zero, + right, − left		Horizontal Range at Shock Arrival	
	Desired	Actual	Desired	Actual	Desired	Actual	Desired	Actual
Lacrosse	5,200	6,751	14,000	13,700	0	200	22,100	28,238
Zuni	33,300	34,029	17,000	16,900	0	−1,750	93,100	—
Erie	4,400	3,829	10,000	10,450	0	150	12,150	14,006
Flathead	12,600	13,462	26,500	25,700	0	1,900	41,100	44,686
Inca	2,900	2,624	10,000	9,815*	0	−150	10,500	11,392
Dakota	17,800	16,955	18,000	17,650	0	1,600	48,100	43,632
Apache	28,000	28,517	10,000	10,200	0	0	43,000	48,375
Huron	9,400	10,223	16,000	16,200	0	−350	27,500	31,493

* From ground station data.

TABLE 3.3 AIRCRAFT TIME ZERO POSITIONING INFORMATION

Shot	Absolute Altitude	Horizontal Range Aircraft to Ground Zero	Slant Range Aircraft to Ground Zero	Track Offset from Ground Zero + right, − left	True Airspeed	Ground Speed	True Heading	True Course
	ft	ft	ft	ft	ft/sec	ft/sec	deg	deg
Lacrosse	13,700	6,751	15,273	+200	828	817	134	137
Zuni	16,900	34,029	37,995	−1,750	800	807	081	073
Erie	10,450	3,829	11,129	+150	679	681	049	050
Flathead	25,700	13,462	29,012	+1,900	763	754	119	119
Inca	9,815*	2,624	10,159	−150	—	668	—	050
Dakota	17,650	16,955	24,474	+1,600	728	761	123	119
Apache	10,200	28,517	30,286	0	488	492	055	050
Huron	16,200	10,223	19,156	−350	784	775	051	051

* From ground station data.

TABLE 3.4 AIRCRAFT CONFIGURATION AT TIME ZERO, IN DEGREES

Shot	Angle Between Thermal Ray and Horizontal Receiver	Fuselage Angle of Attack +, Nose Up −, Nose Down	Angle Between Thermal Ray and Instrumented Tail Cone Surface	Angle Between Thermal Ray and Instrumented Fuselage Hatch Surface	Angle Between Thermal Ray and Aileron Surface T-56	Angle Between Thermal Ray and Aileron Tab Surface T-60	Angle Between Thermal Ray and Elevator Tab Surface T-28	Angle Between Thermal Ray and Elevator Tab Surface T-2
Lacrosse	63.17	−0.6	96.83	63.17	68.20	69.20	73.00	74.90
Zuni	28.44	−0.4	93.46	28.44	27.36	28.36	32.00	32.10
Erie	68.77	−0.3	88.53	68.77	71.70	72.70	76.34	76.66
Flathead	61.47	+0.3	94.83	61.47	64.60	65.60	69.07	72.17
Inca	—	—	—	—	—	—	—	—
Dakota	45.09	−0.4	91.91	45.09	47.05	48.06	50.96	52.36
Apache	19.24	+1.0	93.11	19.24	23.62	23.62	24.80	25.30
Huron	57.59	−0.3	98.71	57.59	76.27	77.27	80.20	80.00

TABLE 3.6 AIRCRAFT SHOCK TIME POSITIONING INFORMATION

Shot	Absolute Altitude	Horizontal Range Aircraft to Ground Zero	Slant Range Aircraft to Ground Zero	Track Offset from Ground Zero + right, − left	True Air Speed	Ground Speed	True Heading	True Course
	ft	ft	ft	ft	ft/sec	ft/sec	deg	deg
Lacrosse	13,700	28,238	31,451	1,150	830	819	134	135
Zuni	—	—	—	—	—	—	—	—
Erie	10,480	14,006	17,297	−150	684	702	049	053
Flathead	28,700	44,685	51,873	1,300	724	716	119	119
Inca	9,815	11,392	14,619	−200	—	667	—	047
Dakota	17,650	43,652	47,066	2,300	722	763	123	122
Apache	10,200	45,376	46,464	0	453	475	056	060
Huron	16,200	31,493	35,418	100	727	748	061	061

TABLE 3.7 AIRCRAFT CONFIGURATION AT SHOCK TIME

Shot	Gross Weight	C.G. Location	Wing Tank Fuel	Fuselage Angle of Attack +, Nose Up −, Nose Down	Angle Between Gust Vector and Horizontal Receiver
	lb	pct M.A.C.	lb	deg	deg
Lacrosse	34,060	25.1	1,000	−0.6	27.56
Zuni	37,006	23.5	900	−0.4	—
Erie	37,165	24.6	0	−0.3	36.76
Flathead	38,215	25.4	0	+0.3	33.50
Inca	—	—	—	—	—
Dakota	37,515	23.9	0	−0.4	24.37
Apache	41,115	25.6	1,000	+1.0	15.12
Huron	38,090	24.6	0	−0.3	29.66

TABLE 3.9 REPORTED METEOROLOGICAL CONDITIONS

Haze condition to 20,000 ft present for Lacrosse detonation. Zero haze for all other events. Albedo of 0.6 used in all cases.
Cloud Type Symbols: C = Cumulus; AS = Altostratus; CS = Cirrostratus; AC = Altocumulus; SC = Stratocumulus.

Shot	Wind Direction and Speed at Aircraft Altitude	Ambient Temperature at Sea Level	Ambient Temperature at Aircraft Altitude	Ambient Pressure at Sea Level	Ambient Pressure at Aircraft Altitude	Visibility at Sea Level	Water Vapor Pressure at Sea Level	Clouds 1/10 Quantity C Cloud Type at 1.5 - 4.0 Layer Height ft × 10^3 N.T. No Type Given
	deg/knots	F	F	psi	psi	sta mi	mm Hg	
Lacrosse	110/5	81.0	36.86	14.626	8.670	10+	22.8	1/10 C at 1.5 - 4.0, 1/10 AS at 18.0 - 19.0, 5/10 CS at 43.0 - 44.0
Zuni	105/10	81.0	24.0	14.66	7.904	8	21.7	4/10 AC at 8.0 - 12.0, 6/10 AS at 17.0, thin layer, 4/10 C at 25.0 - 27.0
Erie	85/4	80.3	51.08	14.635	10.070	10+	21.7	1/10 C at 1,500 - N.T., 2/10 AC at 19.0 - 20.0
Flathead	170/15	82.0	10.46	14.690	5.450	10	23.0	4/10 SC and C at 2.0 - N.T., 10/10 CS at 30.0 - N.T.
Inca	—	93.3	—	14.645	—	10+	23.6	2/10 C at 1.8 - 5.0 to 8.0, 10/10 CS at 23.0 - >30.0
Dakota	190/8	82.0	19.67	14.635	7.430	10+	22.4	3/10 AS at 12.0 - N.T., 7/10 CS at 35.0 - N.T.
Apache	140/18	80.3	47.12	14.635	10.150	10+	22.2	2/10 C at 1.5 - 2.5, 2/10 SC at 2.0 - 4.0, 8/10 CS at 30.0 - 35.0
Huron	60/13	81.4	30.38	14.616	7.960	10	23.1	3/10 C at 1.8 - 10.0 to 15.0, 10/10 CS at 30.0 - N.T.

Figure 3.1 Sample calorimeter and radiometer time histories.

Pages 37+38 deleted

3.5 SHOT SEMINOLE

The aircraft was withdrawn from this event after it was learned that this detonation was of a special nature and that the effects would be unpredictable.

3.6 SHOT FLATHEAD

The B-57B aircraft participated in this event and obtained recorded data successfully. The aircraft was offset to the right of the desired course line about 1,900 feet at time zero and 1,300 feet at time of shock arrival. In addition, due to rough air, the aircraft oscillated about the roll axis during the thermal pulse. No visible damage occurred to the aircraft.

3.7 SHOT BLACKFOOT

Shot Blackfoot occurred at Eniwetok Atoll at the same time that Shot Flathead occurred at Bikini. A comparison of the preshot information available concerning these devices indicated that the probability of the desired effects from Shot Flathead was greater than that from Shot Blackfoot. Therefore, Shot Flathead participation was chosen and the aircraft was withdrawn from Shot Blackfoot.

Figure 3.6 Sample time history of wing torque and aircraft cg acceleration.

3.8 SHOT KICKAPOO

The B-57B aircraft was withdrawn from this event because the information available concerning the expected yield from this detonation indicated that the desired inputs to the aircraft could not be obtained.

3.9 SHOT INCA

The aircraft participated as scheduled. The MSQ-1A positioning system operated successfully throughout the mission. No recorded data other than film badge readings were obtained from this event, because the recording equipment was inadvertently turned off prior to takeoff.

No visible damage to the aircraft resulted from this test. Ground observation placed the actual time of shock front arrival equivalent to the predicted value but there were no recorded data available to determine the accuracy of this observation. The aircraft was positioned for the limiting gust loads.

3.11 SHOT MOHAWK

This mission was aborted due to the malfunctioning of the MSQ positioning equipment.

Pages 41+42 dele

3.13 SHOT NAVAJO

The aircraft was withdrawn from this test because the pilot was grounded for medical reasons.

3.14 SHOT TEWA

The aircraft was withdrawn from this event because analyses of the information available for this detonation indicated that the participation in this test would not add significant data to that previously obtained.

3.15 SHOT HURON

Chapter 4
DISCUSSION

The following sections discuss the weapon effects, aircraft responses and delivery capability of the B-57B resulting from the data collected during Operation Redwing.

4.1 THERMAL INPUTS

In order to determine the reliability of the methods for predicting thermal effects in space, the relationship between weapon yield and thermal inputs must be determined. The results presented in Chapter 3 are measured values of this relationship. The values of effects found by the analytical methods were compared with the measured data. In addition, measured parameters were used in all formulas to predict effects so that these values could be compared with the measured effects. The following sections present these comparisons and discuss their significance.

4.1.1 Total Thermal Radiation Normal to a Horizontal Receiver (Q_e). The measured values of Q_e, obtained from calorimeters placed in the aft hatch of the B-57B, were compared with the computed value obtained by analytical methods. The results are presented in Table 4.1 and Figure 4.1.

Some diffusion across the quartz domes may have occurred where the angle of incidence was large, and the resulting measured values may indicate slightly smaller inputs than those which actually existed. In the cases of Shots Huron and Flathead, 90-degree field-of-view calorimeters were used to obtain the data, and the total reflected radiation may not have been seen by the calorimeters. In addition, during Shot Flathead participation the aircraft rolled back and forth and was offset from the desired track during the thermal phase which fact may have further reduced the readings obtained for this event. During Shot Erie, only one calorimeter operated in the aft hatch.

All computed values of Q_e were greater than the measured values. This condition is more desirable than being unconservative since overestimation of conditions results in an additional margin of safety for the aircraft.

Considering all available information, correlation between measured and computed Q_e appears relatively good, and the analytical methods (see References 7, 9, and 10) are considered sufficiently accurate for computing thermal radiation inputs to a horizontal receiver as applied to the B-57B.

4.1.2 Total Thermal Radiation Normal to Receiver Looking Directly at Burst Point (Q_s). The measured values of Q_s were obtained from calorimeters located in the tail cone of the B-57B and aimed directly at the burst point. The comparison of values of Q_s was conducted in the same manner as the comparisons in the preceding section. The plot of measured versus computed Q_s is presented in Figure 4.2. Numerical values of measured and computed Q_s and and their numerical percentage differences are shown in Table 4.2.

As in the preceding section, percentage differences between the measured and computed values appear to be misleading when small inputs are considered; hence, numerical differences and the plot of measured versus computed values will be used for discussion.

Generally, the tail cone calorimeter readings were considered more reliable than those of the aft hatch. There is less chance of diffusion of the thermal radiation when the calorimeters are aimed directly at the burst. Although 90-degree field-of-view calorimeters had to be

relied upon for most of the measured data, it is believed that the instruments described closely the true thermal inputs provided the fireball remained nearly centered in the field of view. The motion pictures showed: (1) the tail cone was aimed directly at the fireball during all participations except in Shot Flathead, where the aircraft was offset from the desired track and (2) that rolling occurred during the thermal phase of the detonation permitting the fireball to move off center of the field of view of the calorimeters. This resulted in measured inputs being lower than actual inputs.

An analysis of the motion pictures obtained during Shot Apache participation showed clear evidence of broken cumulus clouds between the burst point and the aircraft during the thermal phase. Since the computation method did not account for attenuation by clouds, this fact no doubt resulted in a greater difference between the predicted and measured values than would generally be the case.

The films of the Shot Zuni participation also showed some clouds between the burst and the aircraft. The formation consisted of broken cumulus clouds which were much less dense than those present during Shot Apache. As in the Apache participation, the difference between the predicted and measured values should be expected to be greater than under clear-sky conditions. However, the clouds were so thin that only a small increase of attenuation should be noted.

Regarding Figure 4.2 and Table 4.2, it can be seen that the differences between the measured and computed values of Q_s for Shots Zuni, Flathead, and Apache are, in fact, greater than the differences noted for the remaining detonations. It may also be noted that the shots just listed are in the order of increasing differences between measured and computed values. This is the order expected from the foregoing discussion of these three detonations.

As in the case of Q_e, all computed values of Q_s are greater than the measured values. This

Figure 4.1 Measured versus computed thermal radiation normal to horizontal receiver, Q_e.

Figure 4.2 Measured versus computed thermal radiation normal to receiver looking at fireball, Q_s.

condition is desirable for the reason noted in the preceding section.

The correlation between measured and computed values of Q_s was considered relatively good. The present method of computing thermal radiation incident on a receiver normal to the slant ray between the burst point and the receiver (see References 7, 9, and 10) is considered sufficiently accurate as applied to the B-57.

4.1.3 Time-to-Peak-Thermal Pulse (t_{max}). Measured values of the time-to-peak-thermal pulse were obtained from the oscillograph records of the B-57B aircraft. Comparison of measured values with the computed values was conducted in the same manner as in the preceding sections. The plot of measured versus computed t_{max} is presented in Figure 4.3. Numerical values of measured and computed t_{max} and their numerical and percentage differences are presented in Table 4.3.

The correlation between measured and computed values of t_{max} is considered excellent. Numerical differences are small, averaging approximately 0.05 second.

Figure 4.3 Measured versus computed time to peak thermal pulse, t_{max}.

Figure 4.3 shows the excellent correlation between measured and computed values.

With the aircraft on an outbound heading from ground zero at time zero, it is desirable for the computed values of t_{max} to be less than the measured values. This condition is noted for four of the shots. In the remaining three, the reverse is true. This fact indicates that, in those three shots, the effect would reach the aircraft sooner than expected which would result in the aircraft being closer to the burst point and experiencing correspondingly higher inputs. The maximum error in t_{max} would only place the aircraft about 50 feet nearer the burst than expected, however, and the increase in the thermal radiation receiver would be negligible.

The method for computing time-to-peak-thermal pulse (see References 7, 9, and 10) is considered reliable.

4.1.4 Maximum Irradiance (H_{max}). The maximum irradiance was measured by radiometers located in the tail cone of the B-57B aircraft. The comparison of measured and computed values of H_{max} was performed as in the preceding sections. Figure 4.4 presents a plot of measured versus computed H_{max}. Table 4.4 presents the numerical values of measured and computed H_{max} and their numerical and percentage differences.

With the exception of the Shot Erie comparison, correlation was good between computed and measured values of H_{max}. For this reason the existing analytical method (see Reference 10) is considered adequate as applied in this report.

4.2 GUST INPUTS

The three effects associated with the shock wave recorded on the B-57B aircraft were the time of arrival of the shock front, the overpressure, and the duration of the positive phase of the shock wave. The material velocity, the gust direction, and the peak material density were not measured. Since these values are required in the dynamic analysis for determining limiting values of the material velocity, the computed values were found by substituting measured inputs in the relationships developed in Reference 12. The resulting values of total gust, the vertical and horizontal components of the gust, the gust direction, and the peak material density are presented in Table 4.5.

4.2.1 Time of Arrival of Shock Front (t_{sa}). The time of arrival of the shock front at the B-57B aircraft was obtained from the oscillograph records. The measured values were then compared with computed values found by the analytical methods (see Reference 13). The meas-

ured versus computed t_{sa} plots are presented in Figure 4.5. Table 4.6 presents the numerical values of computed and measured t_{sa} and their numerical and percentage differences.

The correlation between the measured and predicted values of t_{sa} was excellent. Numerical differences were all less than one second. The average error was less than two percent. The greatest percentage deviation was in Shot Erie where the computed value was approximately seven percent greater than the measured value. In view of the speed range of the B-57B aircraft, an error in prediction of t_{sa} within plus or minus one second is permissible. No changes in the present method of t_{sa} prediction (see Reference 13) are indicated.

Figure 4.4 Measured versus computed peak thermal intensity, H_{max}.

As in the case of t_{max}, it is desirable that the computed values of t_{sa} be less than the measured values. However, in the three detonations where the reverse condition resulted, the differences were insignificant.

4.2.2 Peak Overpressure in Shock Wave (ΔP_s).

Page 50 Deleted

For the reason described in the sections concerning thermal radiation, it is desirable that the computed values be greater than the measured values.

The method for computing peak overpressure (see Reference 18) is considered sufficiently accurate for use in weapon delivery studies of the B-57B aircraft.

4.2.3 Duration of Positive Phase of Shock Wave (t_p). Measured values of the duration of the positive phase obtained from the oscillograph records were compared with computed values obtained by the anlytical method of Reference 13.

Plots of measured versus computed t_p are presented in Figure 4.7. Table 4.8 shows the numerical values of measured and computed t_p and their numerical and percentage differences. The correlation between computed and measured t_p is considered satisfactory. The average

Figure 4.6 Measured versus computed peak overpressure.

numerical difference was approximately 1.4 seconds and the average percentage difference was approximately 20 percent. In Shots Huron and Flathead the computed values were excessively greater than the measured data with numerical differences being about 2.5 seconds. For the remaining detonations, differences were on the order of one second or less.

The duration of the positive phase was used in the dynamic analysis for predicting the gust response of the B-57B airframe. In the analysis used, the response was not particularly sensitive to small errors in t_p. For this reason and because the errors in t_p prediction indicated worse conditions than those which actually existed, the present method of computing t_p (see Reference 13) is considered satisfactory for use in the dynamic response studies of the B-57B.

4.3 THERMAL RESPONSE

With respect to thermal radiation, the B-57B was limited by the temperature of the aileron tabs with the elevator tabs being very near critical. Also the 0.040 skin and the 0.032 skin components are near critical with respect to thermal stress. The test aircraft was instru-

mented with thermocouples at various locations on these components to get the temperature rises and the overall temperature distribution. To verify the thermal analysis, the measured thermal response of the aircraft was then compared with the theoretical response using measured input data.

4.3.1 Basic Data and Method for Temperature Calculations. The midpanel skin temperatures on the instrumented surfaces were recalculated using the final yields, weather data, and measured inputs. The method used to calculate these temperatures is described in Reference 7. The heat inputs to the aircraft for these calculations were the average of the calorimeter readings measuring the vertical component of the thermal radiation as shown in Table 4.1. These values were used to determine the equivalent incident thermal radiation using the aircraft altitude and its horizontal range from ground zero. Components of this radiation were then taken for the particular angle of each skin panel calculated. This was done since the slant range thermal radiation and its vertical component do not have a direct geometrical relationship, and the skin panels in question were very near the horizontal. The ambient air temperature used was taken from weather balloon data, since the aircraft outside-air-temperature instrumentation picked up boundary layer effects. The Mach numbers used were calculated from the aircraft instrumented airspeed and weather balloon atmospheric data. The skin panel angles were determined from the aircraft geometry, average recorded control surface positions (the aileron and aileron tab angles were assumed to be the same as those of the wing except in Shots Huron and Apache where the aileron angles were recorded), average recorded aircraft pitch, and the

Figure 4.7 Measured versus computed duration of positive phase, t_p.

theoretical angle of attack for 1-g flight. The absorptivities used for the jet black lacquer were for the particular incident angle of the heat rays as presented in Reference 2. For the exception when the tabs were painted gray, an absorptivity of 0.55 was used. The perpendicular value of the absorptivity was checked at various times during the Operation Redwing tests and little variation was found. The specific heat of the skin was taken as 0.22, an average for the temperature range involved. The heat capacity of the paint was taken as 0.0013 Btu/ft^2 - deg F as determined by post Operation Redwing laboratory tests conducted on coupons cut from the upper skin of the aileron tab. The paint heat capacity was included in the analysis but its effect was negligible.

Since absorptivity values obtained by reflectance techniques cannot account for the insulating and energy storing characteristics of the paint layer, these absorptivity values introduce significant errors in skin temperature rise computations. In an effort to reduce these errors, the thermal irradiance method of absorptivity was developed. This method consists of irradiating the test surface with a calibrated source (500 watt photoflood lamps with a 3,360 F color temperature) so that the exact incident energy is known. The temperature-time history of the surface is recorded and by studying its cooling characteristics, after the source has been turned off, a decay constant for that particular surface can be determined. This decay constant contains all three cooling factors, convection, conduction, and radiation, since it is actually obtained from the temperature-time history of the specimen.

Using this decay constant, the peak temperature rise is corrected to determine the temperature rise which would have been measured if there had been no heat losses. The energy absorbed by the metal skin is then calculated using this corrected temperature rise and the absorptivity is found by dividing the energy absorbed by the energy incident. The methods and equipment developed for measuring absorptivity by the thermal irradiance method have been tested in the laboratory and on Operation Redwing and have been shown to be reliable, repeatable, and accurate to within a probable error of ± 5 percent. It has also been shown that a significant amount of energy may be stored in the paint layer and never cause a rise in temperature of the metal portion of the panel. It is concluded that the absorptivity values obtained on painted panels by the thermal irradiance method define more accurately that portion of the incident energy causing a temperature rise in the panel than does a method depending upon the measurement of reflected energy.

4.3.2 Comparison of Measured and Predicted Temperatures. The measured versus calculated temperature data are presented in Figures 4.8 through 4.10. All of the measured data for the points calculated have been plotted even though some of the recorded values appear to be in error when compared with near-by values. These were not deleted since no reason other than test data scatter is apparent. The average of the points for all of the shots indicates the theoretical temperature to be approximately 15 percent conservative. The recorded temperatures on the aileron tab, the critical surface, vary from 70 percent to 107 percent of the predicted values and average approximately 86 percent for all shots. A detailed inspection of the aileron tab after the Operation Redwing tests revealed that a potting compound had been used

when the thermocouples were installed on the tab (Reference 2). This would impose a heat sink in the area of the thermocouples. Also, the tab temperatures during Shots Apache and Huron were recorded by thermocouples spot-welded externally to the skin. In this case the thermocouple wire, protruding in the boundary layer upstream of the thermocouple junction, most likely caused abnormal boundary layer heat transfer, and since the thermocouples were exposed directly to the radiation, the exact temperature is questionable. For these reasons, the recorded temperature of the aileron tab should be interpreted with caution.

The predicted temperatures on the elevator tab (not quite as critical as the aileron tab) appear to be much more reliable than those of the latter and give a better indication of the applicability of the theoretical analysis. The recorded temperatures vary from 86 to 98 percent of the predicted values with an average of 92 percent for all shots.

Figure 4.8 Measured versus computed temperatures of aileron and aileron tab.

4.3.3 Analysis. Some of the factors in the analysis which may contribute to conservatism are: differences of the actual pulse shape from the normalized pulse used in Reference 7, the boundary layer heat transfer coefficient, and the assumptions that the reradiation and internal convective cooling were zero. All factors except the boundary layer heat transfer coefficient were considered negligible. The boundary layer coefficients were determined from the skin temperature time-histories following the end of the heat pulse and were compared to the theoretical values. These comparisons indicated the coefficients to be approximately 10 percent conservative; however, the effect on the peak temperatures was less than 5 percent conservative. Other factors which may have added to poor correlation were burning of the paint and inaccuracies in the measured data (Reference 2). The exact effect of burning the paint was unknown,

but it was expected to absorb heat from the skin thus making the analysis appear conservative. The heat inputs affected the peak temperature rises proportionately; and scatter in the calorometer readings indicated that these inputs probably varied at least by a few percent (Reference 2). The angles of the skin panels with respect to the incident heat rays also had a great effect on the temperature rises especially in shots where this angle was small. For these shots a small change in the angle produced a large change in the component perpendicular to the skin panels.

4.3.4 Thermal Damage. Thermally induced damage consisted of minor paint burning on Shot Zuni and severe paint burning, skin buckling, and material properties reduction (see Reference 2), such as reduction in yield point, modulus of elasticity, and also initial stages of delamination of the fiber glass in the radome. No special absorptivity configuration was used in these shots to obtain high inputs to specific aircraft components. The entire aircraft was painted with standard B-57B paint (jet black lacquer). Therefore, the entire aircraft, not just a few components, was subjected to the thermal inputs as an actual operational aircraft would have been.

Figure 4.9 Measured versus computed temperatures of elevator and elevator tab.

The paint was burned only slightly on the aileron tabs and elevator tabs during Shot Zuni.

erature rise. Above approximately 420 F the paint charred severely, melted, and outer layers rolled off and blew away (Figures 4.7 through 4.11). The perpendicular absorptivity of the paint after it was burned did not change appreciably.

Figure 4.10 Measured versus computed temperatures of stabilizer.

Permanent material properties reduction become appreciable above 400 F, but this fact was not readily detectable at the test site. Therefore, tensile tests were conducted at the Martin Company in November 1956 on coupons cut from the upper and lower surfaces of the aileron tab used in Shots . These test results showed 54,000-psi yield and 73,000-psi ultimate for the upper surface and 50,000-psi yield and 67,500-psi ultimate for the lower surface. This data indicated a reduction in material properties on the heated surface; however, these values did not approach the minimum guaranteed values used in design. It must be remembered that for this material, natural aging would occur and that the material

properties may have been partially restored in the interval between the detonations and the laboratory tests.

4.3.5 Summary. The results of the Operation Redwing tests show the thermal analysis and limits to be reasonable and practical for use in determining the delivering capabilities of the B-57B.

The temperature limit of 400 F on the 0.032 and thinner skin which was set before the test was verified by the results of the test. The critical surfaces (the tabs) could withstand considerably higher temperatures safely if buckling were permissible. However, the 0.032 skin surfaces reached their ultimate much quicker when 400 F was surpassed, as the flaps appeared to be the most critical of these surfaces during the Operation Redwing tests. The safety factor for an all-black B-57B is slightly more than 1.5 with the 400 F limit on the tabs.

From correlation with the test data, the temperature analysis (see References 7, 9, and 10) appears to be conservative. Boundary layer theory is such that only approximate solutions can be made practically, and improvements in boundary layer theory would make a smaller change in the final temperatures. Knowing the measured values, heat input, absorptivity, and the corresponding angle accurately for each skin panel would improve the correlation greatly.

Measured heat inputs by laboratory standards were subject to an error of ± 10 percent. This accuracy could hardly be expected during field operations. The perpendicular component of the heat input onto the surface in question had to then be obtained by using the measured input and the corresponding angle. Precise determination of the angle was important since slight variations of this value caused a wide scatter of computed temperatures. The accuracy of this determination was affected by the exactness in fixing a location, consideration of the fireball as a point source, and the aircraft roll, pitch, and yaw attitudes.

Another factor entering into the temperature computation was the surface absorptivity. The values used were those of controlled laboratory specimens, disregarding the presence of any surface film (dust, dirt, moisture) as might be encountered during a test. Variation of the absorptivity with angle was also determined from theoretical curves, (the above-mentioned difficulties in determination of the angle were involved).

These factors appeared to be the greatest source of error in predicting the temperatures, since they were difficult to measure during the tests and could be predicted only approximately for an actual operational case. It is doubtful if much refinement could be made in predicting the temperatures without complicating the analysis and measuring system greatly. Such complications would be unjustified since the results were within the accuracy of predicting the environment.

4.4 GUST RESPONSE

The participating B-57B was instrumented to record accelerations, bending moments, shears, and torques on various aircraft components (Figures 3.7 to 3.9 and Table 3.1) in order to define the response of the aircraft to gust inputs.

Data obtained at Wing Stations 78 and 166 and Stabilizer Station 24.5 were used for comparison of measured and predicted gust response.

The aircraft weight condition during Shot Lacrosse consisted of a heavy wing and a very light fuselage fuel condition (approximately 5,000 lbs less than that used in the dynamic analysis). The light-weight fuselage condition would tend to increase the effect of the fuselage motion on the stabilizer loads. Accelerometers were installed on the wing to aid in the definition of the wing vibratory modes. Wherever possible, the gross weight simulated the light-weight wing fuel condition utilized in dynamic analysis. The fuselage gross weight was higher in this condition, thereby lessening the fuselage effect on stabilizer loads.

The structural gust shear loads measured on the wing during Shot Lacrosse were 67 percent of the predicted load. The wing torque predictions were unconservative but not critical. The stabilizer measured bending moment was 2.5 times the predicted gust load. Examination of the time-history measurements indicated that the fuselage vibratory modes could significantly af-

fect the stabilizer loads. In addition, the higher stabilizer vibratory modes were present.

The Shots Erie, Flathead, and Dakota wing-gust-load measurements were generally 20 percent conservative as compared with the calculated loads. Although the measured stabilizer bending moment loads were from 1.5 to 2.0 times the predicted loads, the wing loads remained critical.

The measured fuselage bending moments for the first four detonations were approximately 3.5 times the predicted loads. The higher fuselage loads principally resulted from the coupling effects between the fuselage and stabilizer vibratory modes. An additional fuselage station was instrumented to measure fuselage vertical bending at Station 472 and an additional accelerometer was added to aid in the definition of fuselage loads and vibration. Even though the fuselage predicted loads were so greatly underestimated, there was a sufficient margin in the allowable load to eliminate considering the fuselage as a critical component.

Although a good position was obtained during the Shot Inca participation, no gust data were obtained because of failure of the recording instrumentation system. Based on actual yields and the aircraft position at t_{5a}, the aircraft received loads of 77 percent of the design limit load at the critical wing station. This included a load reduction due to the general conservative trend of the predicted wing loads.

During Shot Apache, a large horizontal gust component was experienced. As indicated in Reference 8, paragraph 3.1.1.g, this produced an alleviating effect on the structural gust loads; therefore the measured wing loads were lower than predicted. During Shot Apache, the wing

TABLE 4.9 COMPARISON OF MEASURED AND COMPUTED WING STRUCTURAL LOADS

All values are the ratio, measured load/predicted load.

Shot	Wing Bending Moment						Wing Shear				Wing Torque			
	Wing Station 78		Wing Station 166		Wing Station 256		Wing Station 78		Wing Station 166		Wing Station 78		Wing Station 166	
	Gust Load	Total Load	Gust Load	Total Load	Gust Load	Total Load	Gust Load	Total Load	Gust Load	Total Load	Gust Load	Total Load	Gust Load	Total Load
Lacrosse	0.40	0.69	0.40	0.64	0.50	0.73	0.67	0.84	0.39	0.69	1.75	1.17	1.90	1.13
Erie	0.77	0.88	0.84	0.90	0.62	0.77	0.82	0.88	0.80	0.91	1.20	1.11	3.28	1.79
Flathead	0.81	0.90	0.54	0.73	0.65	0.81	0.93	0.99	0.85	0.93	2.42	1.56	3.20	1.59
Dakota	0.58	0.72	0.74	0.82	0.72	0.82	0.70	0.82	0.68	0.80	1.92	1.48	2.30	1.46
Apache	0.13	0.54	0.24	0.57	0.27	0.64	0.21	0.54	0.15	0.51	0.54	0.97	0.69	0.88
Huron	0.48	0.67	0.49	0.66	0.53	0.66	0.61	0.78	0.50	0.67	1.15	1.09	2.15	1.39

was in the heavy fuel condition at the time of shock arrival. The aircraft gross weight was 1,000 pounds heavier than in the analysis condition.

Shot Huron measured data indicated 20 percent conservatism as compared to the wing computed loads. The measured stabilizer load was 1.75 times the predicted bending moment.

Figures 4.11 and 4.12 indicate the correlation of the measured and predicted loads. Data from Shots Lacrosse and Apache are omitted from these figures as a result of the gross weight and horizontal gust considerations outlined above. The ratios of measured to predicted incremental and total structural loads on the wing for all detonations are indicated in Table 4.9. The stabilizer and fuselage ratios are presented in Table 4.10. A tabulation of wing and stabilizer loads at the critical stations is contained in Table 4.11.

The allowable gust velocities at the critical component locations, as determined at the standard conditions of Reference 8 were 26 ft/sec for the wing (Station 123, shear) and 67 ft/sec for the stabilizer (Station 141, bending moment).

If the allowable gust velocities are adjusted by use of the ratio between the measured and predicted loads, the gust velocities are adjusted by use of the ratio between the measured and predicted loads, the gust velocities given in Table 4.12 are allowed, based on 100 percent design limit load.

The results indicate that the light-weight aircraft could be positioned closer than originally predicted. The results of Shot Lacrosse indicated that the stabilizer may become critical for some aircraft weight conditions.

The critical components on the aircraft were determined by means of limit design envelope

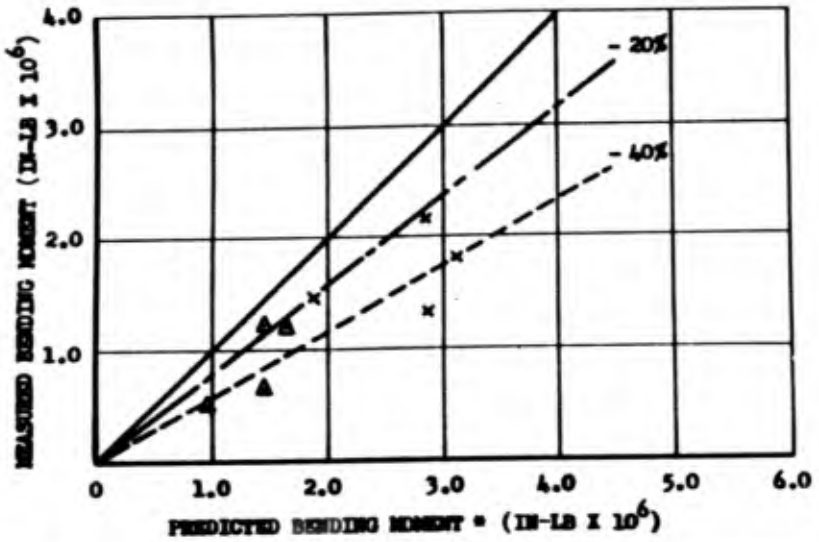

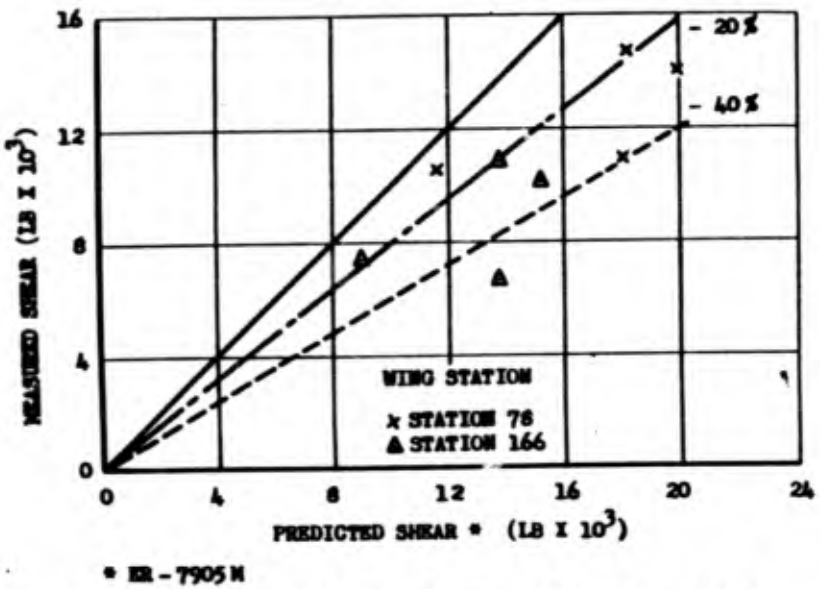

* ER-7905 M

Figure 4.11 Measured versus computed wing gust loads.

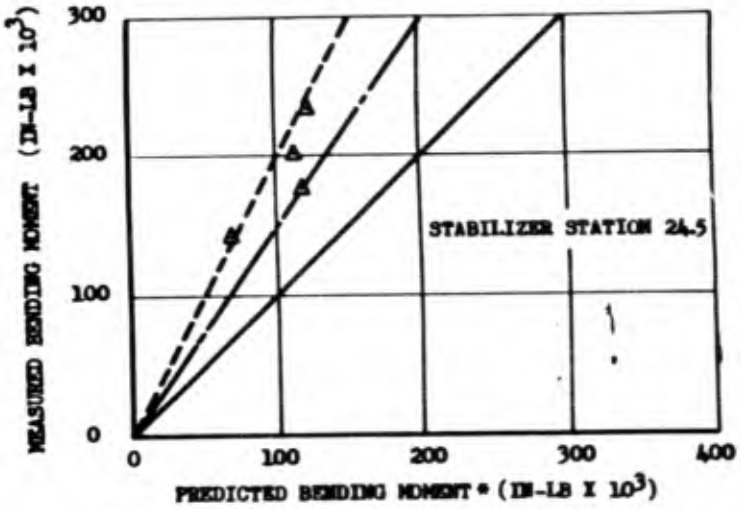

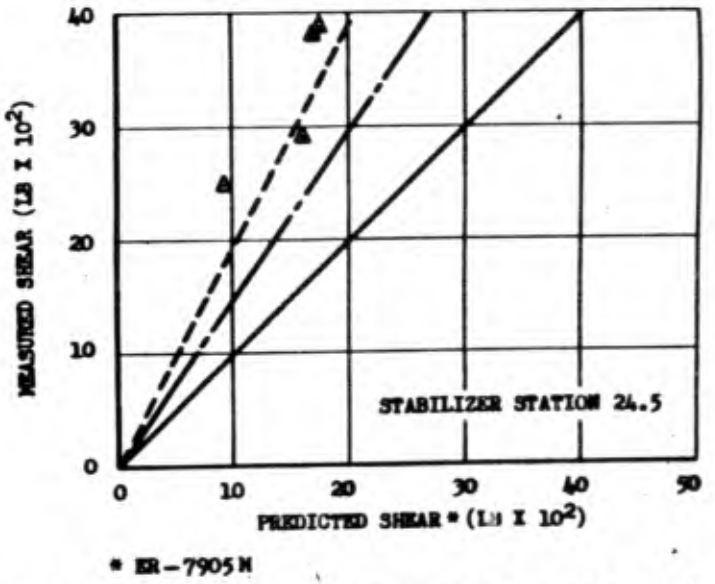

* ER-7905 M

Figure 4.12 Measured versus computed stabilizer gust loads.

data. Following the field program, an examination of the structural data available from analyses and static tests indicated that use of the structural limit curves for the wing would generally permit higher gust velocities. In the final Air Force Technical Report (Reference 1) the structural limits were utilized.

Due to the unconservatism of the stabilizer predicted loads, new blast analyses were conducted on a limited basis before and after the completion of the field program. These analyses investigated the following effects: (1) higher frequency stabilizer modes, (2) various forcing functions, (3) gust duration, and (4) effects of gust penetration. Results of these investigations are discussed in Reference 1. No additional wing analyses have been conducted to determine the effects for other gross weights.

4.5 OVERPRESSURE RESPONSE

The highest overpressure the B-57B experienced during the tests was 1.06 psi during Shot Apache. Since the aircraft can withstand overpressure of 2.0 psi without permanent deformation, no visible damage or adverse effects to the structure were either expected or experienced. Overpressures approaching the engine critical limits were not attained.

4.6 NUCLEAR RADIATION

The Shot Inca device was the only one in which the nuclear radiation required careful scrutiny. Until this time, the aircraft was positioned to receive approximately one rem or less from each detonation, so that the radiation limit would not be exceeded. In the preceding

events, the one rem positions were not limiting and gust remained the limiting factor. It was desired that gust loading be limiting for this event also. The total radiation received up to this time was 1.15 rem from Shots Lacrosse and Erie.

TABLE 4.12 ALLOWABLE GUST VELOCITIES

	Measured Load* / Predicted Load	Adjusted Allowable Gust Velocity ft/sec	Measured Load† / Predicted Load	Adjusted Allowable Gust Velocity ft/sec
Wing‡	0.76	34	0.93	28
Stabilizer§	1.77	38	2.01	34

* Determined from average obtained from Shots Erie, Flathead, Dakota, and Huron results.
† Determined from maximum obtained from Shots Erie, Flathead, Dakota, and Huron results.
‡ Using shear at Wing Station 78.
§ Using bending moment at Stabilizer Station 24.5.

The nuclear radiation readings obtained from film badge dosimeters worn by the pilot of the test aircraft were plotted against the computed values and are presented in Figure 4.13. The 45-degree line indicates the ideal case in which the computed and measured values are identical.

Only the pilot's film badge readings were used for this comparison, since the observer's film badge readings were consistently about two-thirds the value of the pilot's badge readings. This phenomenon was also noted with the sampler B-57B aircraft. The computed nuclear radiation values, the pilot's film badge readings, the observer's film badge readings, and the numerical and percentage differences between the pilot's readings and the computed values are presented in Table 4.13. It should be noted that only three shots are listed in the table. In the remaining shots no nuclear radiation was expected and none was received.

No final explanation for the pilot's radiation dosage being greater than the observer's dosage has been found at this time. Suggested explanations of this phenomenon include: (1) shielding of the observer from some of the direct radiation by the aircraft structure and the fuselage fuel tanks, (2) shielding of the observer from the scattered radiation of which a greater portion was received by the pilot through the windshield, or (3) a combination of the above. The correlation between the computed radiation values and the pilot's film badge readings tended to indicate that the pilot's readings were more representative of the actual conditions.

Figure 4.13 Measured versus computed total gamma radiation, γ, received by pilot.

Two of the computed values were less than the measured values. Generally, this is undesirable, since underestimation of conditions to be received by the aircraft reduces the margin of safety desired.

The present methods of predicting nuclear radiation on aircraft flying away from a nuclear detonation appear to be sufficiently accurate over the range of radiation values received by the B-57B during Operation Redwing. However, the data are insufficient for either confirming present analytical methods (Reference 13) or indicating if any changes are required.

Chapter 5
CONCLUSIONS and RECOMMENDATIONS

From the data obtained by the participation of Project 5.4 in Operation Redwing, the following conclusions and recommendations can be made.

5.1 CONCLUSIONS

The participation in Operation Redwing provided sufficient information for the determination of the aircraft's delivery capability, thereby satisfying the primary objective of this project.

The responses of the critical components of the B-57B aircraft to the inputs of a nuclear detonation were less than predicted. Therefore, the weapon delivery capability of the B-57B aircraft is better than the capability described in the B-57B Phase I-1 and Phase 1-A Special Weapons Studies.

The existing methods of predicting weapon inputs and aircraft responses, although in some cases unconservative, generally tend to be conservative but are considered satisfactory for predicting the B-57B delivery capability.

The data obtained by the participation of the B-57B in Operation Redwing will provide: (1) valuable design criteria data for future aircraft and (2) a basis for the verification and/or correction of present methods of predicting weapon effects in space and on aircraft structures.

5.2 RECOMMENDATIONS

It is recommended that no further participation of the B-57B be planned for the purposes of defining its weapon delivery capability.

It is further recommended that the data collected by this project be used to refine the present methods of predicting weapon effects in space and on aircraft structures.

REFERENCES

1. WADC TR 57-97; (draft manuscript); Wright Air Development Center, Dayton, Ohio.

2. "B-57B Operation Redwing Data"; WADC TN 56-465, October 1957; Wright Air Development Center, Dayton, Ohio; Secret.

3. W.J. Bonner; "B-57B Phase 1-A Special Weapons Study"; Report No. ER 7772, 21 April 1956; The Glenn L. Martin Company, Baltimore, Maryland; Secret Restricted Data.

4. "B-57B Phase 1-1, Special Weapons Study"; Report No. ER 8218, 25 May 1956; The Glenn L. Martin Company, Baltimore, Maryland; Secret Restricted Data.

5. A. Ambrosio, B. Bussel, and W. F. MacInnes; "Temperature Distribution in a Typical Aircraft Structure Due to Transient External Heating"; WADC TR 52-216, April 1953; Wright Air Development Center, Dayton, Ohio; Unclassified.

6. P.W. Boone; "Effects of Short Time Exposure to Elevated Temperatures on Mechanical Properties of 24ST Aluminum Alloy"; Engineering Laboratories Progress Report No. 47-25, 22 July 1947; The Glenn L. Martin Company, Metals Research and Development Group; Unclassified.

7. J.W. Cox; "Allowable Thermal Inputs for the B-57B from Special Weapons Heating"; Report No. ER 7276, 1 June 1955; The Glenn L. Martin Company, Baltimore, Maryland; Secret Restricted Data.

8. "A Method for Determining the Dynamic Response and Resulting Loads on a B-57 Airplane Due to Blast Effects"; Report No. ER 7905, January 1956; The Glenn L. Martin Company, Baltimore, Maryland Secret.

9. R.M. Chapman, and M.H. Seavy; "Preliminary Report on the Attenuation of Thermal Radiation from Atomic or Thermonuclear Weapons"; AFCRC TN 54-25, November 1954; Air Force Cambridge Research Center, Bedford, Massachusetts; Secret Restricted Data.

10. J.W. Saylor, Jr., 1st Lt USAF, L.C Pincus, 1st Lt USAF; "Generalized Procedure for Determining Thermal Radiation at a Point in Space"; WADC TN 55-266, August 1955; Wright Air Development Center, Aircraft Laboratory, Dayton, Ohio; Secret Restricted Data.

11. "Capabilities of Atomic Weapons"; TM 23-200, November 1957; Armed Forces Special Weapons Project, Washington, D.C.; Confidential.

12. G.J. Frasinelli; "The Effects of Atomic Explosions on Aircraft", Vol VII, Supplement; WADC TR 52-244, Vol VII, 1 March 1953; Wright Air Development Center, Dayton, Ohio; Secret Restricted Data.

13. R.I. Epstein; "B-57 Redwing Field Manual"; Report No. ER 7990, 15 January 1956; The Glenn L. Martin Company, Baltimore, Maryland; Secret Restricted Data.

14. E.A. Witmer, N.P. Hobbs, and J.C. Loria; "Resume of Effects of Very High Yield Atomic Explosions on Aircraft Structures – Explosion Characteristics, Structural and Aeroelastic Blast Effects, and Thermal Radiation Effects"; WADC TR 54-386, MIT, 10 August 1956; Wright Air Development Center, Dayton, Ohio; Secret Restricted Data.

15. C.B. King, and J.F. Schell; "The Technique of Peak Temperature Measurement with Temp-Tape"; Memorandum Report No. 125, March 1956; University of Dayton, Division of Research, Dayton, Ohio; Unclassified.

16. C.W. Blechschmidt, M. Daniels, and P. Kimmel; "Instrumentation and Airloads Calibration Program for B-57B Redwing"; Report No. ER 7812, November 1955; The Glenn L. Martin Company, Baltimore, Maryland; Unclassified.

17. W. Womack; "In-Flight Calibration of Wing Airload Strain Bridges"; Report No. ER 7812, Appendix C, November 1955; The Glenn L. Martin Company, Baltimore, Maryland; Unclassified.

18. J.R. Alexander; "A Modified Method for Computing of Overpressure and Overpressure Envelopes"; AFTN-WCIS-55-13, May 1955; Secret Restricted Data.

Pages 67+68 deleted